Journal of Geography and Geology; Vol. 17, No. 1; 2025
ISSN 1916-9779 E-ISSN 1916-9787
Published by Canadian Center of Science and Education

Fate of the Santo Cristo de Burgos Galleon or Beeswax Wreck (1693): Impacts from High-Energy Neotectonic, Oceanographic, and Geomorphic Processes, Manzanita-Nehalem, Oregon, USA

Curt D. Peterson[1], Scott S. Williams[2], Thomas G. Mock[3] & Carl A. Whiting[3]

[1] Department of Geology, Portland State University, Portland, Oregon, United States

[2] Maritime Archaeological Society, Astoria, Oregon, United States

[3] Nehalem Valley Historical Society, Manzanita, Oregon, United States

Correspondence: Curt D. Peterson, Geology Department, Portland State University, Portland, OR., 97207, United States. Tel: 1-503-730-9266. E-mail: curt.d.peterson@gmail.com

Received: November 22, 2024 Accepted: January 10, 2025 Online Published: January 27, 2025

doi: 10.5539/jgg.v17n1p1 URL: https://doi.org/10.5539/jgg.v17n1p1

Abstract

The fate of the Santo Cristo de Burgos galleon (1693) is established from 1) alongshore dispersals of shipwreck artifacts prior to the 1700 Cascadia earthquake, 2) shipwreck artifacts deposited by 1700 tsunami surges in beaches and estuary wetlands, and 3) post-1700 subsidence catastrophic beach retreat in the Manzanita-Nehalem study area. Shipwreck structures, unabraded sherds, and historically salvaged beeswax blocks and tropical wood timbers, are associated with the 1700 tsunami overtopping of the Nehalem Bay sand spit. However, a rapid ship breakup and alongshore dispersal of shipwreck debris must have occurred during the 7 years between the loss of the galleon and the 1700 great earthquake and associated nearfield tsunami surges. The pre-1700 alongshore distribution of recovered artifacts argue for a primary shipwreck site located offshore of the Nehalem Bay sand spit. Measured ocean beach tsunami runup, including high-velocity flow (8 m elevation) likely resulted in further dismemberment of shipwreck superstructures and remobilization of shipwreck flotsam to elevated dune ramps and the over-washed sand spit. Inshore tsunami runup elevations in the lower bay wetlands (3.5 m elevation) and upper bay floodplains (2.7 m elevation) permitted shipwreck flotsam dispersal to reach up-channel distances of 14 km. Catastrophic beach retreat (130 m landward of modern beaches) following the 1700 coseismic coastal subsidence (~1.0 m) would have further eroded beached shipwreck structures. However, backwashed ceramic artifacts could have been initially buried by accommodation space filling (≤1.0 m) in the innermost shelf. Subsequent storm wave remobilization of buried sherds and their transport to headland bounded shoreline entrapments continues to the present. The rapid breakup and pre-1700 alongshore dispersal of the Beeswax Wreck debris, could explain the lack of remaining shipwreck structures for two other lost galleons, the San Agustín (1595) and San Juanillo (1578), on the high-energy central west coast of North America.

Keywords: Santo Cristo de Burgos, Beeswax Wreck, nearshore processes, tsunami surges, beach erosion, dune burial

1. Introduction

Three galleon wreck sites in the central West Coast of North America (Figure 1A) are characterized by widely distributed artifacts but no apparent remains of intact shipwreck hulls (Williams and Junco, 2023). The three galleon shipwrecks are the Santo Cristo de Burgos (1693) near Manzanita Oregon, the San Agustín (1595) in Drakes Bay, California, and San Juanillo (1578) near Esmeralda, in the Baja California Peninsula, Mexico. The focus of this article is on the most northern galleon wreck, the Santo Cristo de Burgos or Beeswax Wreck (Williams et al., 2018). In this article, the fate of the Beeswax Wreck is established from the relationships between 1) coastal landforms, 2) artifact dispersal by alongshore transport, 3) artifact protection by tsunami surge remobilization, and 4) artifact preservation by dune sand or bay mud burial. The relative sequence and timing of these processes are used to test a hypothesis of very rapid breakup and alongshore dispersal of the Beeswax Wreck flotsam, shortly followed by nearfield tsunami remobilization of shipwreck debris to protected overwash settings. The study results presented in this article demonstrate the broader importances of integrating geology,

oceanography, and historical geography with maritime archaeology to better understand early historic shipwreck sites in high-energy sandy coastlines around the world.

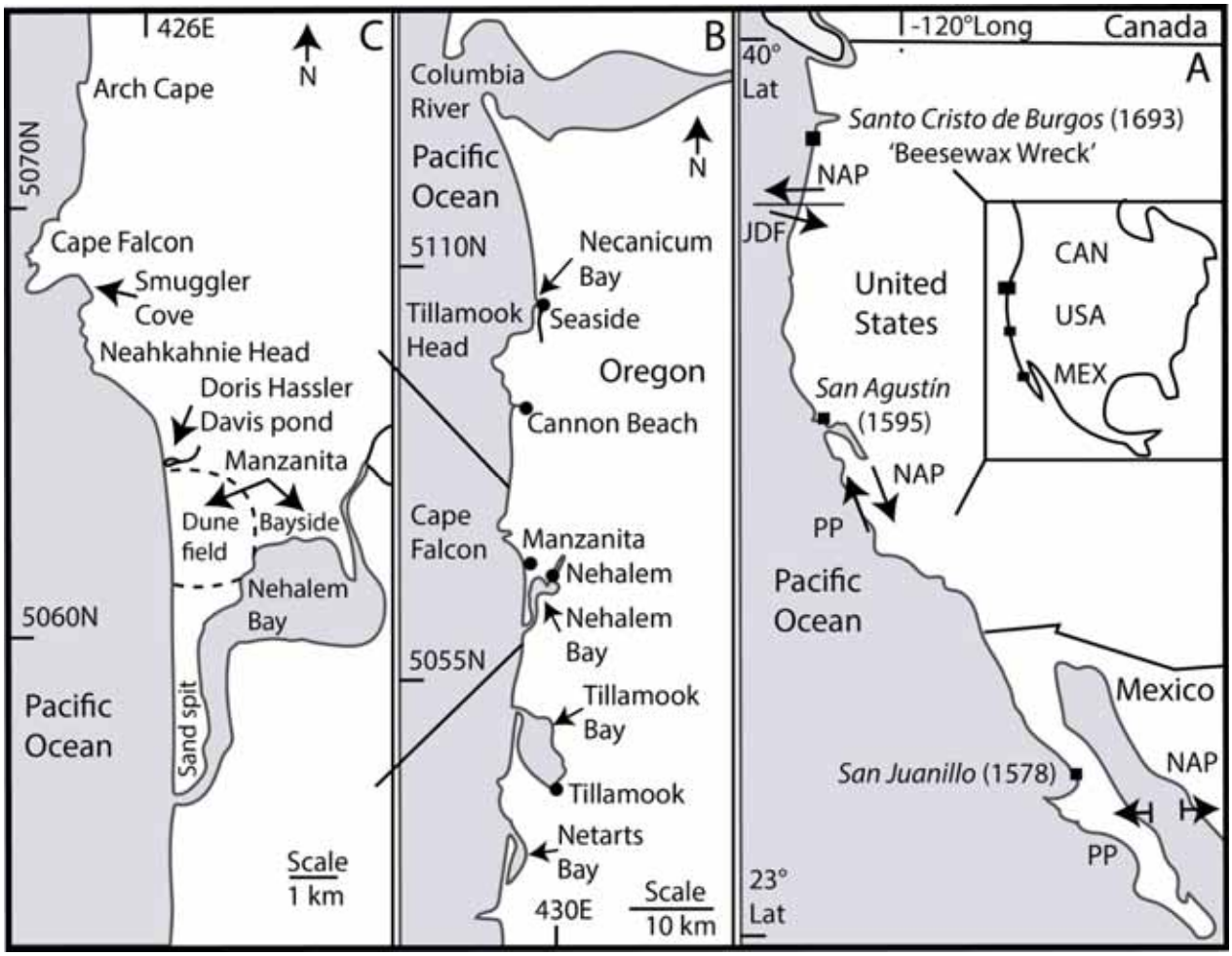

Figure 1. Maps of the study region and study areas

Part A, map of central West Coast of North America showing three reported galleon shipwreck localities including Manzanita, Oregon, and Drakes Bay, California, in the United States, and Esmeralda, Baja California Peninsula, Mexico (solid squares). Coordinates are in degrees Latitude and Longitude. Part B, northern Oregon coast study region. Map coordinates are in 1000 meters UTM 10N Easting and Northing. Part C, study area geomorphic features including the Manzanita dune field and fronting beaches, the Nehalem Bay sand spit, the Manzanita Bayside wetlands, the Doris Hassler Davis Pond, and Smuggler Cove. Map coordinates are in 1000 meters UTM Easting and Northing.

For generations intriguing artifacts from the northern Oregon have spawned coast legends, treasure hunts, a Hollywood adventure film, and documentaries about a shipwreck (Hult, 1968; Marshall, 1984; La Follette et al., 2018; CNN, 2022; OPB 2023). However, no intact ship hull has been recovered. Nehalem tribal oral traditions speak about an early shipwreck on or near the Nehalem Bay sand spit (Figure 1B). Importantly, this shipwreck could have constituted a first contact between the Native Americans and any surviving castaways, including Europeans and East Asians, on the Northwest Coast (Gibbs, et al., 1970; Erlandson, et al., 2001). Between 2006 and 2012, a volunteer research team was assembled to discover the origins of the shipwreck, named the Beeswax Wreck (Williams, 2007; Williams, et al., 2017). This moniker derives from abundant beeswax blocks that were collected by Native Americans and European settlers on 1) the Nehalem Bay sand spit, 2) the beaches fronting the Manzanita dune field, and 3) the Nehalem Bay tide lands (Figure 1C). The preserved artifacts, including stamped beeswax blocks, Asian porcelain sherds, and tropical wood timbers, were traced to the longstanding Spanish Galleon trade (Williams et al., 2018). A widespread dispersal of shipwreck artifacts across the Nehalem Bay sand spit (0.5–1.0 km width and 5 km length) was associated with the coeval emplacement of cobble sheets by the last Cascadia nearfield tsunami in 1700 (Satake et al., 1996; Peterson et al., 2011). The fact of near-term remobilization

of these shipwreck artifacts by the tsunami surges dated the shipwreck to the recorded loss of the Santo Cristo de Burgos in 1693 (Williams et al., 2018). The heaviest iron debris, including the galleon's cannons and anchors, have not been recovered.

For the past 17 years, intensive efforts by various field teams have been focused on locating an intact hull or large structural remnants of the wrecked Santo Cristo de Burgos galleon (Williams, 2023). Searches were conducted onshore and offshore of the Nehalem Bay sand spit, as well as the Manzanita beaches, and the nearby Smuggler Cove (Figure 1C). Those searches were based on 1) early historic accounts of shipwreck structures on the Nehalem Bay sand spit (Clarke, 1899; Williams, 2007), 2) alongshore distributions of collected beeswax and porcelain and earthenware sherds (Figure 2A, B) (Lally, 2008; Litzenberg, 2022), and most recently 3) the discovery of Beeswax Wreck timbers (Figure 2C) in the nearby Smuggler Cove (Peterson, et al., 2023; Williams, 2023). However, neither onshore magnetic surveys nor offshore acoustic surveys located evidence of an intact hull or large remnant structures of the Beeswax Wreck. The wreck of the Santo Cristo de Burgos joins two other galleon shipwrecks on the west coast of North America (Figure 1A) that have left dispersed artifacts, yet no intact lower ship hull or other very large structures (Williams and Junco, 2023). The other two Galleon shipwrecks, the San Agustín (1595) and either the San Juanillo (1578) occurred respectively, in the vicinities of Drakes Bay, California, USA (Meniketti, 2023; Russell, 2023), and Esmeralda, Baja Peninsula, Mexico (Von der Porten, 2019; Von der Porten, 2023; Williams and Von der Porten, 2023).

Figure 2. Scaled artifacts recently collected from the Beeswax Wreck

Part A, Stamped beeswax block, collected from the Manzanita Beaches and now displayed at the Nehalem Valley Historical Society Museum, Manzanita, Oregon (scale card 9 cm total width). Part B, porcelain sherd SC2023 (7 cm wide), collected by one of these authors (Whiting) from the Nehalem Bay sand spit in 2023 (scale bar 3 cm total width). Part C, Beeswax Wreck tropical timber from Smuggler Cove (#4 in Peterson, Williams &, Andes, 2023) with cut holes, square notches, and internal metal fittings (scale card 8.5 cm total width). The timber is currently archived at the Columbia River Maritime Museum, Astoria, Oregon (length 222 cm, dry weight 74.8 kg).

Porcelain sherds and shaped points have been reported from multiple Native American midden sites in the northern Oregon study region (Beals and Steele, 1981; Scheans and Stenger, 1990). Some local tribespeople also traded beeswax pieces to the Lewis and Clark expedition at Fort Clatsop at the Columbia River estuary 1805-1806

(Figure 1B) (Williams, 2017). Nehalem tribal oral traditions related that some shipwreck survivors made it to shore (Smith, 1899; Gibbs, Mengarini and Tolimie, 1970). However, the specific number of castaways and their long-term survivals are not known from contemporaneous written records.

In this article, lidar digital elevation models, 1700 tsunami runup strandlines, and catastrophic beach retreat features are used to evaluate the potential for preservation of intact shipwreck hull structures, and to identify settings that could host additional Beeswax Wreck artifacts. These settings include 1) the Manzanita dune field, 2) the Nehalem Bay sand spit, 3) the Manzanita beach-backshore/sand ramps, and 4) the Nehalem Bay wetlands (Figure 1C). Dune soil chronosequences (Birkeland, 1999) are used to further constrain ages of the Manzanita dune field deposits (Erlandson and Moss, 1999) that could establish the net littoral sand transport direction in late-Holocene time (Peterson et al., 2020. Relative dune deposit ages could also identify deposits that could host Beeswax Wreck artifacts. Maximum runup elevations from the 1700 nearfield tsunami surges (Minor and Peterson, 2016) are established from gouge core transects in a Manzanita beach barrage pond and a Nehalem Bay wetland. Projected tsunami runup elevations and mapped post-subsidence beach retreat features (Peterson et al., 2011) are used to target preserved beach-backshore/dune ramp settings that could host buried shipwreck structures.

Analyses of the alongshore distributions of different shipwreck artifacts are used to constrain the timing and rates of the Santo Cristo de Burgos breakup and artifact dispersal in this high energy coastal setting. These study results also shed light on the fates of the other two lost Spanish galleons, the San Agustin in California (Russell, 2023) and the San Juanillo in Baja California, Mexico (Von der Porten, 2019) that were shipwrecked in the high-energy Pacific Coast of North America (Williams and Junco, 2023).

2. Background

2.1 The 1700 Great Cascadia Earthquake and Tsunami Surges

The Beeswax Wreck study area occurs in a convergent subduction zone margin (Figure 1A). This differs from the San Austin shipwreck, located in a transform plate boundary margin and the San Juanillo, located near a divergent plate boundary margin. Only the Beeswax Wreck study area experiences cycles of nearfield tsunami surges and regional coastal subsidence (Figure 3). By astonishing coincidence, the Beeswax Wreck (1693) occurred just 7 years before the 1700 Cascadia earthquake and associated tsunami surges (Peterson et al., 2011). High energy storm surf could have initiated shipwreck breakup (Peterson et al., 2023), but shortly thereafter the tsunami surges remobilized some shipwreck debris to higher ground beyond the reach of storm waves (Williams et al., 2018). Longer lasting coastal subsidence also impacted the shipwreck debris by processes of catastrophic beach retreat (Peterson et al., 2011) and possible offshore transport of some ceramic sherds. Gradual interseismic coastal uplift during the following centuries then reversed some of the littoral sand supply to onshore. The shoreward sand supply permitted beach progradation and foredune burial of remaining artifacts along the ocean shorelines. Although some of the processes impacting the Beeswax Wreck have been previously identified, they have not been sufficiently quantified to predict remaining artifact distributions.

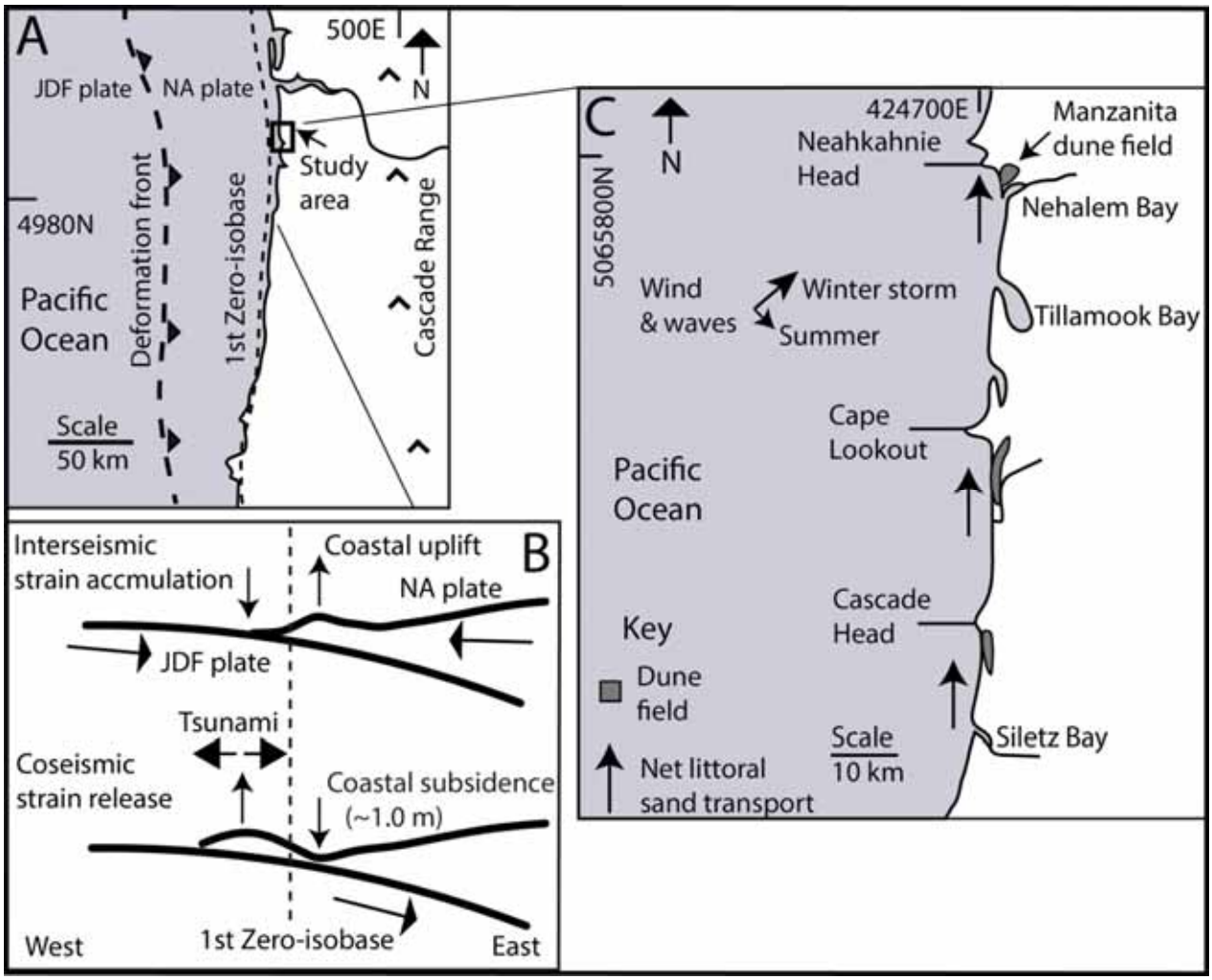

Figure 3. Neotectonic and net littoral sand transport in the study area

Part A, map of the Study Area (boxed) in the central Cascadia subduction zone, including the Juan De Fuca (JDF) plate descending below the North American Plate (NAD) at the deformation front (large, dashed line). The 1st zero-isobase (small, dashed line) is extrapolated offshore of the study area. Figure is redrafted from Peterson and Cruikshank (2014). Part B, diagram of upper-plate flexure, reversing on either side of the 1st zero-isobase, during interseismic stain accumulation and coseismic strain release cycles. Coseismic subsidence and associated abrupt sea level rise is estimated to be ~1.0 m in the study area (Nelson et al., 2020). Associated nearfield tsunami surges are generated by the coseismic uplift, occurring seaward of the 1st zero-isobase. Part C, map of three littoral subcells in the study region, which are bounded by headlands (named) and associated Holocene dune fields (shaded). The strong asymmetries of the dune field distributions demonstrate net-northward littoral sand transport (arrows) in the littoral subcells.

2.2 Alongshore Littoral Sand Transport

Dispersals of Beeswax Wreck artifacts occur over alongshore distances of at least 10 km in the study area (Williams et al., 2018), but the primary shipwreck site has not been identified (Williams, 2023). Nor is it known how much time was required for shipwreck breakup and alongshore dispersals of various types of artifacts. Some of these questions might be addressed if the net directions of artifact alongshore transport could be established. Driftwood accumulations have been observed to occur at the north ends of some littoral subcells in the study region, but the alongshore transport of bedload materials, including sand and gravel, has been debated. A recent mineralogical study (Peterson et al., 2020) refuted the assumption that the abundant sand supply to the study region's beaches and dunes was largely sourced from the large Columbia River (Figure 1B). That sand mineralogical finding is consistent with earlier work that showed upland dune fields of Holocene age to be developed at the south sides of north bounding headlands (Figure 3C) (Peterson et al., 2009). However, the ages

and durations of beach sand supplies to some of the smaller headland bounded upland dune fields have only been dated at reconnaissance levels (Erlandson and Moss, 1999). If northward littoral sand transport is confirmed by youngest dune sand supply to the Manzanita dune field, then historic littoral sand transport can be assumed to be dominated by southwest winter storm winds and waves. Similarly, long term dispersals of some ceramic sherds, since the 1700 tsunami surges, might follow suit and help to explain the disproportionate distribution of recent sherd collections in the study area (Lally, 2008; Litzenberg, 2022).

2.3 Shipwreck Structure and Debris Dispersal from the Beeswax Wreck

Shipwreck structures were reported by early settlers (1850s-1926) to have occurred near or on the Nehalem Bay sand spit (Figure 1C) (Clarke, 1899; Smith, 1899; Vaughn, 2004; Giesecke (2007). Beeswax blocks and tropical wood timbers from the Beeswax Wreck were retrieved from 1) the interior deflation plains of the Nehalem Bay sand spit and 2) the elevated beach backshore/dune ramp surfaces located landward of the Manzanita beaches. Some 6–20 tons of beeswax are reported to have been salvaged from the dispersed shipwreck debris in the study area for commercial purposes, starting in the mid-1800s (Williams 2017; Williams et al., 2018). By the early 1900s, salvaging of the shipwreck timbers had become profitable. Timber salvaging exceeded 10 tons, as extrapolated from reported shipwreck timber haulage by one settler family. The family used horse pulled wagons to haul about one ton of 'teak' wood from about one kilometer of sandy coastline at Manzanita, Oregon in the 1930s (Paul See, pers. comm., 2008). The shipwreck structures/timbers were historically reported to be found along the full length of sandy coastline from the Nehalem Bay tidal entrance to the Manzanita Beaches, about 10 km in length. Total ship structure and cargo hardwood likely exceeded 2,000 tons (Peterson et al., 2023). We estimate that less than 5 percent of the shipwreck timber was recovered. The time interval encompassing the loss of the Santo Cristo de Burgos (1693), the distribution of Beeswax Wreck flotsam artifacts along the sandy beaches, and the January tsunami inundation in 1700 (Satake et al., 1996), is short (7 years). If the initial shipwreck occurred in the Nehalem Bay sand spit area, then such a short interval infers a rapid break-up and alongshore transport of the Beeswax Wreck debris flotsam, possibly within just a few winter storm seasons. In contrast, to buoyant materials such as beeswax and shipwreck timbers, no porcelain sherds were observed in the 1700 tsunami runup deposits from beach backshores/dune ramps observed north of the Nehalem Bay sand spit in the 1930s (Paul See, pers, comm., 2008).

Driftwood timbers from the Beeswax Wreck were recently discovered on a narrow intertidal wave-cut platform and associated sea caves located along the north side of Smuggler Cove (Figure 2C) (Peterson et al., 2023). The North Smuggler Cove (NSC) site is located 8 km north of the Nehalem Bay sand spit (Figure 1C). The mapped Beeswax Wreck timbers (n=27) from the NSC site are interpreted to have been buried and preserved by rockslides. Several lines of evidence suggest that the rockslides at the NSC site were triggered by the last great Cascadia earthquake in 1700. Therefore, the interpreted duration of time between the loss of the Santo Cristo de Burgos (1693) and the 1700 coseismic rockslide burial of the wreck driftwood timbers in Smuggler Cove is short. The northward transport of shipwreck timbers around the large Neahkahnie headland (~1.5 km seaward projection) was rapid, possibly occurring within just a few winters after the breakup of the Beeswax Wreck.

Blocks of beeswax from the Beeswax Wreck were recovered by settlers of European descent from beaches and bays located north of Smuggler Cove in the late 1800s and early 1900s (Williams et al., 2018). Beeswax blocks were collected as far north as the mouth of the Columbia River (Swan, 1857) located 60 km north of the Manzanita study area (Figure 1B). Wreck flotsam artifacts reaching the large Columbia River mouth could have been transported offshore of the large river mouth by riverine/ebb tide currents. Well offshore, they wreck flotsam could have been more widely dispersed, north and south, by ocean winds, waves, and currents.

3. Methods

The location(s) and current condition(s) of the Beeswax Wreck have been unresolved for 150 years (Williams, 2023). To resolve these mysteries the fate of the Beeswax Wreck is divided into five steps in this article. The first step is to establish the net alongshore transport of shipwreck flotsam and bedload transported ceramic sherds by nearshore wind, waves, and currents. The distributions of larger shipwreck structures and unabraded ceramic sherds, as presented in this article, follow an analysis of net littoral sand transport in the study area. The direction and timing of net alongshore sand transport is demonstrated by dune sand accumulation in the Manzanita dune field (Figure 1C). Figurative alongshore reversals of the shipwreck artifact dispersals are then used to constrain the location(s) of the initial shipwreck. The second step is to establish the measured distances and elevations of the 1700 tsunami surge transport of shipwreck flotsam and ceramic sherds across the Nehalem Bay sand spit. Historic photographs, locations of 1700 tsunami gravel deposits, and recent finds of unabraded shipwreck sherds are used together with modern lidar digital elevation models (DEMs) to establish minimum distances and elevations of tsunami remobilized shipwreck artifacts on the ocean beaches and across the sand spit. The third step is to measure

the geologically recorded runup of the 1700 tsunami surges adjacent to the ocean beaches and in the Nehalem Bay estuary. These maximum runups are used to predict the maximum tsunami strandline positions of shipwreck flotsam artifacts in the study area. The fourth step is to evaluate the catastrophic beach erosion distances that resulted from prolonged sea level rise that accompanied the coseismic subsidence from the 1700 Cascadia earthquake rupture (Figure 3). These catastrophic beach retreat distances are used to map the minimum landward positions of tsunami remobilized artifacts that could be protected from winter storm surf erosion. The fifth step is to use reported sites of beeswax block recovery from the Nehalem Bay wetlands to establish the distances and elevations of shipwreck flotsam dispersal in the upper reaches of the estuary. The specific techniques that are used to address the five methodology steps (1–5) above correspond, respectively, to the five Results Sections (4.1–4.5) below.

Satellite images of the Manzanita dune field and the Nehalem Bay sand spit (Figure 1C) were divided into three overlapping sections. The Google Earth Pro satellite imagery (April 15, 2020) was magnified to an eye altitude of 7.8 km (Google Earth Pro, 2023). Bare earth hill shaded lidar images of the study area (3 m spatial resolution) were accessed from the Department of Oregon Geology and Mineral Resources (DOGAMI) lidar viewer (DOGAMI, 2023). The lidar images were scaled to cover three overlapping study area sections, including 1) the Manzanita dune field, 2) the Nehalem Bay sand spit, and 3) the southern end of the sand spit and the Nehalem Bay tidal entrance (Figure 1C) (Peterson, 2024). The lidar elevation data are reported to the nearest 0.1 m elevation relative to the North American Datum (NAVD88). The NAVD88 0-m elevation is equivalent to the mean lower low water (MLLW) or -1.5 m mean sea level (MSL) in the study region.

Apparent dune field advances in the Manzanita dune sheet are interpreted from alignments of parabolic dunes and abandonment of dune precipitation ridges (Cooper, 1958). The ages of the dune field accretions establish whether the latest dune field sand accumulations from net northward littoral sand transport are coeval with the timing of the Beeswax Wreck (first methodology step). Abandoned foredunes in the Nehalem Bay sand spit are interpreted from shore parallel ridges that occur landward of the modern foredunes (Reckendorf et al., 2023). The historic foredunes became stabilized by invasive (non-native) European dune grass, planted in the 1940s and 1950s (Cooper, 1958; Oregon Historical Society, 2024). Due to very limited C^{14} dates from the Manzanita dune field (Moss and Erlandson, 1995) the timing of dune sand supply from the adjacent beaches to the Manzanita dune field is better constrained by dune topsoil profile chronosequences. Dune soil chonosequences reflect the duration of topsoil development during periods of stability under vegetative cover (Birkeland, 1999). The specific topsoil development parameters used here are the presence/absence of the topsoil A-horizons and Bw-horizons, and the averaged unconfined shear strength or pocket penetrometer value (kg cm^{-2}) of the Bw-horizons. These parameters were tested against abandoned foredune topsoil profiles (C^{14} dated) in the nearby Columbia River beach plain (Figure 1B) (Woxell, 1998; Peterson et al., 2006). Representative dune topsoil sites in the Manzanita dune field were profiled in 2022 and 2023 (Peterson, 2024). The topsoil chronosequences reported in this article were developed for the specific conditions in the study region and are only applied in this article for relative dune deposit dating at the reconnaissance level.

Locations of historically reported shipwreck structures (Giesecke, 2007) at the north end of the Nehalem Bay sand spit are supported by interpretations of timber excavation anomalies as recently discovered in a 1939 aerial photograph. Recently collected unabraded porcelain sherds, which were found in association with 1700 tsunami gravel deposits, are mapped and georeferenced for elevation in lidar images from the Nehalem Bay sand spit (second methodology step).

Maximum apparent runup of 1700 tsunami surges were mapped (2024) at a proximal beach barrage pond (Doris Hassler Davis Pond) and at a supratidal wetland of Nehalem Bay (Manzanita Bayside wetlands) (Figure 1C). The extents of recorded tsunami runups (third methodology step) are based on the presence of distinct sandy organic detritus layers. Such layers extend upward and landward of distinct tsunami sand sheets (Peterson et al., 2008). The tsunami origins of the sandy tsunami layers are based on hand lens identification of rounded quartz-rich beach sand. Multiple gouge cores (2.5 cm diameter) were taken several meters apart at each site to confirm the presence or absence of apparent tsunami deposit layers. Representative cores (0.6–0.8 m depth subsurface) were photographed and logged on-site at 1.0 cm depth resolution. Gouge core sites are georeferenced by 12 channel-GPS with ≤5 m estimated potential error (EPE). Core sites were evaluated for elevation using online lidar bare earth elevations (±0.1 m NAVD88) (DOGAMI, 2024). Instrumentally recorded storm surges only reach 1.5 m runup, above predicted tide levels, in the study area (Pittock et al., 1982), so are distinguished from the nearfield paleo-tsunami runups (7–15 m) in the study region (Peterson et al., 2008; Peterson et al., 2015, Minor and Peterson, 2016).

A dune-buried stone feature in the back-edge of the Manzanita beaches, fronting the Manzanita dune field (Figure 1C), was found to be associated with 1700 catastrophic beach retreat scarps (fourth methodology step). Whereas

the retreat scarps were recorded in across-shore ground penetrating radar (GPR) profiles in 2007–2008 (Peterson & Cruikshank, 2007, Peterson et al., 2011), the GPR did not discriminate the buried stone features from hosting sand, due to a lack of resistivity contrast. The dune buried stone features were identified in 2023 as a shore-parallel cobble berm in early historic aerial photos. Detailed mapping of the cobble berm topography was performed by hand auger coring, as completed in 2023. The boreholes were hand augured with a Dormer sand auger (7 cm diameter) at 10–20 m distance intervals along the previously recorded across-shore GPR profiles. Though no cobble samples were returned with the sand auger, the bending of the auger cutting blades (steel) indicated the tops of the cobble berm at the subsurface depths of auger boring refusal. Elevations of the 2023 boreholes surface deposits were established by lidar (DOGAMI, 2023). The catastrophic beach retreat scarps, as imaged in the GPR profiles, were confirmed by both historic photographs and the borehole transects.

Beeswax block sites that have been reported from the Nehalem Bay wetlands are mapped for elevation by lidar to establish minimum tsunami runup elevations in the upper reaches of the Nehalem Bay estuary (fifth methodology step). The most distal site of beeswax collection in the North Fork of the Nehalem River was measured for runup elevation using the stratigraphic depth of beeswax block burial relative to the modern surface elevation, as taken from lidar spot elevation data (DOGAMI, 2024).

4. Results

4.1 Lidar Survey and Soil Chronosequences of the Manzanita Dune Field

The extents of dune surface stabilities and relative emplacement ages of the Manzanita dune field (Figure 1C) are established from successive, but diminishing, episodes of dune field advance up the southern (northward bounding) slopes of Neahkahnie Mountain (Figure 4). The dune sand transgressed upslope from adjacent beaches by dominant southwest wind forcing in the Manzanita dune field. Successively younger episodes of dune field advance are labeled A, B, and C (Figure 4), representing dune emplacement ages of late-Holocene (~5±2 ka), latest-Holocene (~2±1 ka), and very latest-Holocene (~0.5±0.5 ka), respectively. These limiting ages are interpreted from dune topsoil chronosequences or the relative developments of dune topsoil Bw-horizons in soil profile sites (1–7), as shown in Table 1 and Figure 5. Dune surfaces with existing topsoil Bw-horizons could host Beeswax Wreck artifacts at or the near the surface. Dune surfaces with no Bw-horizons, but with intact topsoil A-horizons, could either slightly pre-date or post-date the Beeswax Wreck, and associated artifact emplacements. Dune surfaces without an intact topsoil A-horizon imply historic (post-1700) dune burial, thereby complicating artifact detection in the Manzanita dune field deposits. Catastrophic beach retreat, following the 1700 coseismic coastal subsidence, limits the seaward extent of preserved dune ramp paleosols along the Manzanita beaches. The catastrophic retreat, as initially imaged in GPR profiles 2007–2008 (Peterson et al., 2011), is generally mapped at 130 m landward distance from the modern beach backshore (4 m NAVD88) in Figure 4.

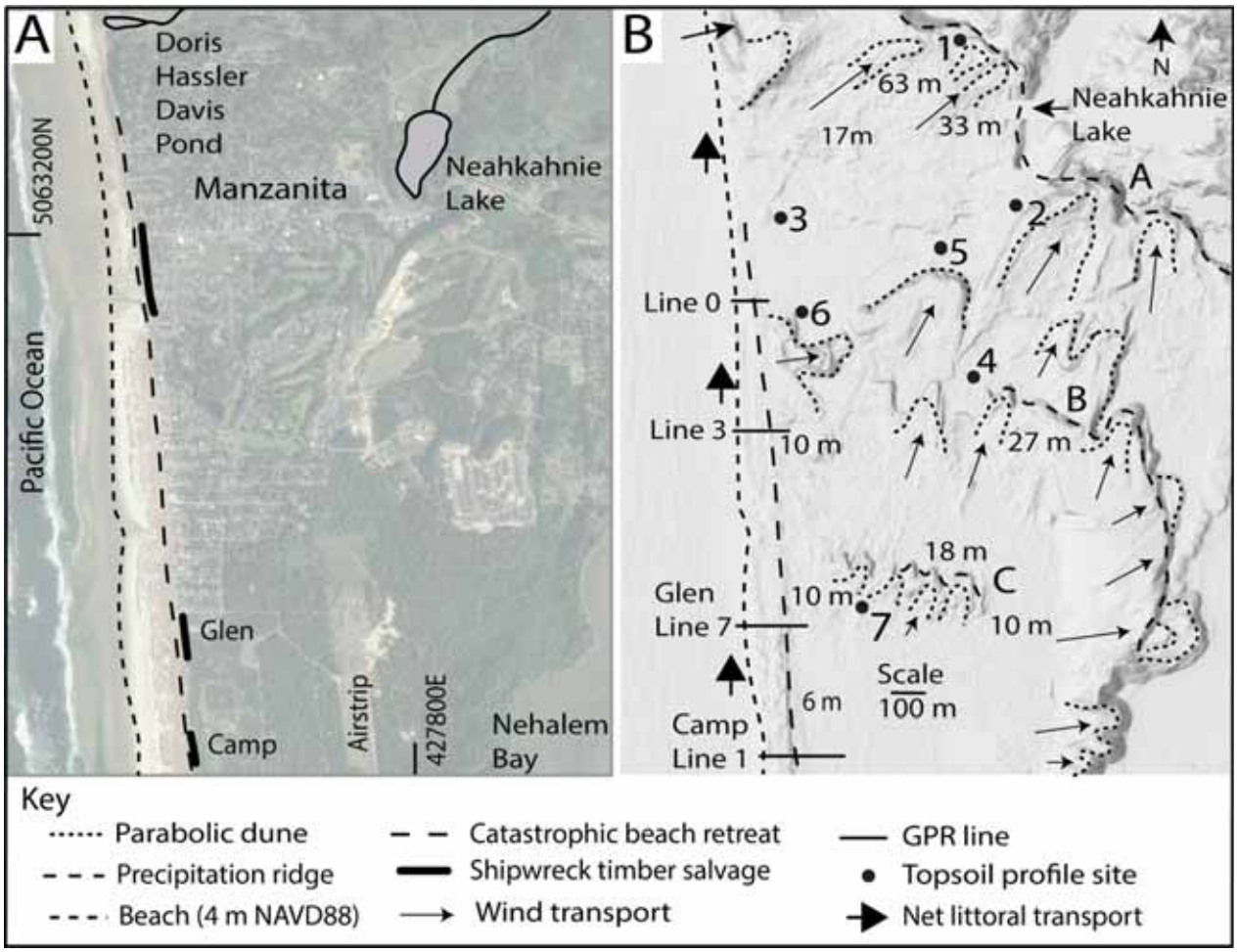

Figure 4. Satellite and hill shaded lidar images of the Manzanita dune field and beaches

Part A, satellite image of the Manzanita dune field and broad sandy beaches, and the north end of the Nehalem Bay sand spit, including modern beach backshore, catastrophic beach retreat scarp, and shipwreck timber salvage areas (Paul See pers. comm., 2028; Giesecke, 2007). Map coordinates are in meters UTM Easting and Northing. Basemap satellite image is from Google Earth Pro (Google Earth Pro, 2023). Part B, lidar bare earth hill shaded image depicting dune features in the Manzanita dune field. GPR lines (2007–2008) that establish catastrophic retreat scarp positions are numbered Lines 0, 3, 7, and 1. GPR lines 7 and 1, respectively, are published as Glen and Camp in Peterson et al. (2011). Dominant wind directions are shown by parabolic dune forms and dune field accretion events (lettered A, B, C). Dune topsoil sites are numbered 1–7. See Table 1 for topsoil profile data. Representative spot elevation data are in meters (m) NAVD88. Base map is from DOGAMI (2023).

Table 1. Topsoil profile data from the Manzanita dune field

Site	UTM-N	UTM-E	A-horizon (cm)	B-horizon (cm)	B-horizon color	Pocket P. (kg cm^{-2})	Age
1	5063814	427527	0-22	22-34	7.5YR 7/6	1.25	3–7 ka
2	5063409	427809	0-18	18-26	5YR 4/6	1.75	3–7 ka
3	5063670	426800	0-10	0	—	—	0–1 ka
4	5062720	427700	0-15	15-18	7.5YR 6/6	0.75	1–3 ka
5	5062017	427486	0-10	10-12	10YR 7/4	0.5	1–3 ka
6	5062608	426980	0-5	0	—	—	0–1 ka
7	5061665	427151	0	0	—	—	Historic

Notes: Topsoil profile site coordinates are in meters UTM Northing and Easting. Soil A (organic-rich) horizons and soil Bw (mineral precipitate) horizons (Birkeland, 1999) are measured in centimeters (cm) of subsurface depth. Soil colors (moist soil) are from Munsell color charts. Dune parent sand is 2.5Y8/4. Topsoil A-horizons are identified by incorporated decomposed (dark) organics. Pocket Penetrometer measurements (Pocket P) are unconfined shear strength (kg cm^{-2}). Dune topsoil ages of 3–5 ka correspond to developed Bw-horizons (> 5 cm thickness) and pocket penetrometer values of >0.75 kg cm^{-2}. Dune topsoil ages of 1–3 ka correspond to incipient Bw-horizons (1–5 cm thickness) and pocket penetrometer values of 0.25–0.75 kg cm^{-2}. Dune topsoil ages of 0–1 ka lack a Bw-horizon, but dune parent soil (C-ox) horizons have pocket penetrometer values of <0.25 kg cm^{-2}. Historic dune topsoil ages correspond to an absence of a topsoil A-horizon. Dune topsoil ages, relative to published chronosequences (Peterson et al., 2006), are 1) late Holocene (estimated 3–7 ka), 2) Latest-Holocene (estimated 1–3 ka), 3) very latest-Holocene (estimated 0–1 ka), and 4) Historic (estimated 0–1700 AD). See Section 3 for topsoil relative dating methods. See Figure 3 for topsoil profile locations in the Manzanita dune field. See Figure 4 for color-coded topsoil profile logs.

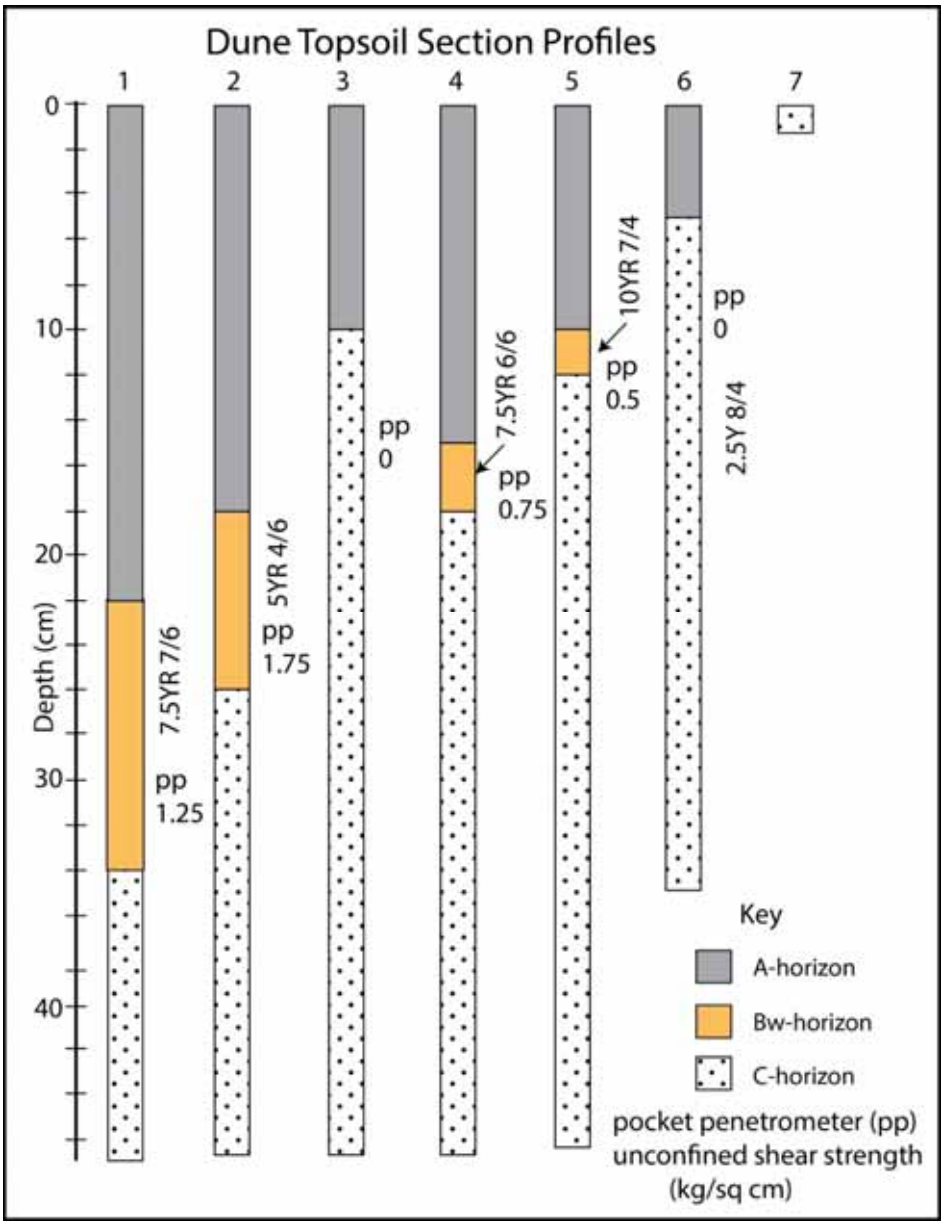

Figure 5. Topsoil profile logs

Profile logs for topsoil sections in the Manzanita dune field. See Figure 3 for topsoil profile locations. See Table 1 for topsoil section profile data. Dune topsoil Bw horizons are identified by orange-yellow color (Munsell colors)

(Birkeland, 1999) and are quantified for relative age based unconfined shear strength or cementation, using a pocket penetrometer (pp) (Peterson et al., 2006).

The successive northward and eastward accretions of dune sand in the Manzanita dune field (Figure 4) demonstrate dominant northward littoral sand transport and sand supply to the dune sheet (5 km^2 surface area) via the adjacent Nehalem Bay sand spit and Manzanita beaches, throughout late-Holocene time (5–0 ka) (Table 1, Figure 5). The net northward littoral sand transport is opposite to that expected due to the southward pointing Nehalem Bay sand spit (Figure1C). The sand spit likely prograded south during summer conditions of onshore beach sand replacement when fair weather waves and winds arrive from the northwest. However, the demonstrated northward dominance of littoral sand transport in the study area must occur during winter storm conditions of southwesterly storm winds and waves. Such conditions are associated with offshore sand displacement and northward directed geostrophic and wave bottom currents (Peterson et al., 2020). Ceramic sherds, traveling as bedload in the nearshore zone, should have been episodically transported northward during major storm events. Shipwreck flotsam, such as shipwreck timbers, should also have been dispersed northward from the wreck site during the dominant southwesterly storm wind conditions (Peterson et al., 2023). Shipwreck timbers were salvaged from the beach backshores or foot slopes of the Manzanita dune field (Paul See, pers, comm., 2008) and from incipient foredune areas at the north end of the Nehalem Bay sand spit in the early 1900s (Figure 4) (Giesecke, 2007). These relations suggest a primary shipwreck site located somewhere along the Nehalem Bay sand spit.

The burial of organic Beeswax Wreck artifacts by transgressive dunes, foredunes and/or reactivated dunes helped to preserve the artifacts, yet it has obscured their locations in late historic time (late 1900s to present). For example, early settler accounts report shipwreck structures to be partially covered by sand in two locations at the northern end of Nehalem Bay sand spit, including Camp and Glen (Figure 6). The Camp site structure, including a section of keel and ribs, was reportedly located about 30 m landward of a natural seawall due west of the Campground (Giesecke, 2007). The seawall is now interpreted to have been a catastrophic beach retreat scarp and/or beach retreat cobble berm (see Section 4.4 below) that forms a nearly straight line along the 1939 shoreline. The Camp location may have been confirmed (2024) by Giorgio Litt and one of these authors (Williams) in their co-discovery of the cut-off remnants of two posts that were said to have been erected in the early 1900s to mark the position of the shipwreck structure (Giesecke, 2007). In the 1939 aerial photograph (Figure 6), the dark anomalies in the barren dune sand, located between the retreat scarp and the Campground D loop, are interpreted to represent possible shipwreck debris and/or excavations by 'teak' timber salvagers. A 2007 GPR profile (Line 1 in Figure 4) from the Camp locality (Peterson et al., 2011) shows the retreat scarp or seawall to be presently buried under 5–10 m of stabilized foredune sand.

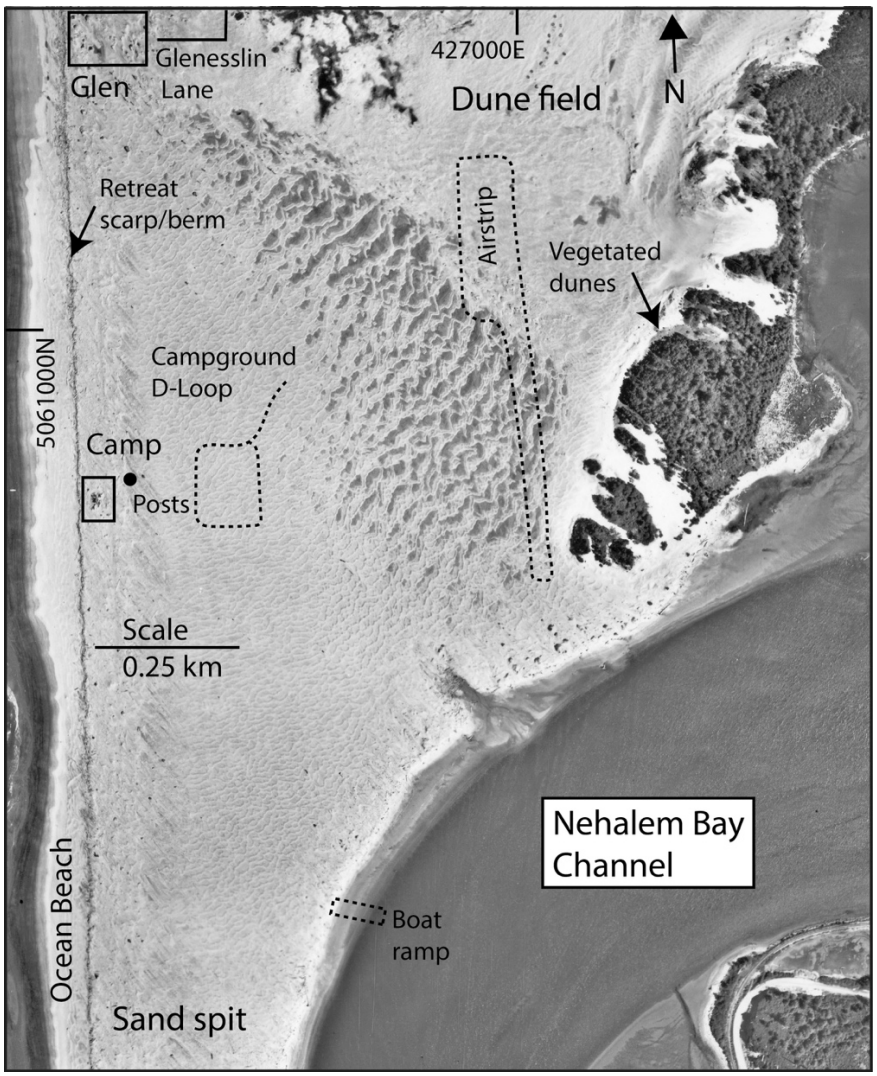

Figure 6. Aerial photograph (1939) of the transition from the Manzanita dune field and Nehalem Bay sand spit

Dark anomalies (boxed) on the ocean side of the sand spit are apparent in the barren beach/dune sand located landward of the beach retreat feature (natural seawall) at two historically reported shipwreck structure sites (Camp and Glen) (Giesecke, 2007). The anomalies are interpreted to represent possible sites of 'teak' timber excavation and salvaging. The Camp site is georeferenced by what might be historically erected posts (Posts at 426970E, 5060750N m UTM) at a reported wreck structure site (Giesecke, 2007). The Glen location is georeferenced by historically recorded wreck structure sightings near the south end of the beach access road, which now terminates at Glenesslin Lane (bold line) (Giesecke, 2007) Modern outlines of the airstrip, the State Park D loop, and the boat ramp are plotted.

The Glen location in Figure 6 had also been identified as a shipwreck structure site from early settler accounts (Giesecke, 2007). Shipwreck structure sections were reported to have been lodged about 20 m landward of the seawall or beach retreat cobble berm, as well as further landward, in the vicinity of what is now Glenesslin Lane. Several dark anomalies, located in the barren dune sand between the beach retreat cobble berm and the seaward end of Glenesslin Lane (Figure 6), appear to represent pits or excavations. Some of the excavations extend below the groundwater surface, as shown by partial flooding of the pits. The sand pits could be the result of 'teak' timber explorations/salvaging that continued through the 1930s. A 2007 GPR profile (Line 7 in Figure 4) from the Glen locality (Peterson et al., 2011) shows the seawall scarp to be presently buried under 5–10 m of stabilized foredune sand. Additional small anomalies, interpreted to have been timber salvage excavation pits (n>50), are scattered 0–250 m east of the retreat scarp, from the Glen locality to south of the Camp locality, as evident by magnification of the 1939 aerial photograph (Figure 6). Small dark anomalies in the 1939 aerial photograph are also scattered along the northeastern bayside of the sand spit, but their origins have yet to be investigated.

4.2 Lidar Survey and 1700 Tsunami Inundations of the Nehalem Bay Sand Spit

Tsunami gravel sheets and Beeswax Wreck artifact flotsam were deposited along nearly the full length and width of the Nehalem Bay sand spit (Figure 7) by the last Cascadia nearfield tsunami of 1700 (Satake et al., 1996; Peterson et al., 2011; Williams et al., 2018). The tsunami deposits occur at elevations reaching 2–6 m NAVD88, located landward of historically stabilized and accreted modern foredunes. A catastrophic beach retreat scarp, resulting from the 1700 coseismic coastal subsidence (Peterson et al., 2011), is mapped under the vegetatively stabilized foredunes. Tsunami transported cobbles and boulders are locally exposed landward of the late historic foredunes. The northernmost observed tsunami boulder (C1), as measured to 34 cm in diameter and deposited at 5 m elevation, is mineralogically traced to the Nehalem River source. The largest observed tsunami boulder (160 kg) was also deposited at 5 m elevation. Its entrainment required a calculated hydraulic shear stress of 100–250 N m^{-2} (Chambliss et al., 2012) from high velocity flow, probably ≥1 m water depth. Surge runup heights over the spit interior were ≥6 m elevation. The sand spit transitions northward to the upland dunes of the Manzanita dune field at ~10 m elevation at the north end of the airstrip (Figure 4). No tsunami debris deposits were observed in the upper 1.5–2.0 m depth subsurface at the north end of the airstrip (Williams and Peterson, 2017). For this article the maximum tsunami surge strandline at the north end of the sand spit is tentatively placed under the 8 m NAVD88 elevation contour, as mapped in Figure 7B. The lowest tsunami cobble sheet elevations (2–3 m) on the east side of the central sand spit might reflect 1700 spit surface downcutting by localized tsunami scour (see below).

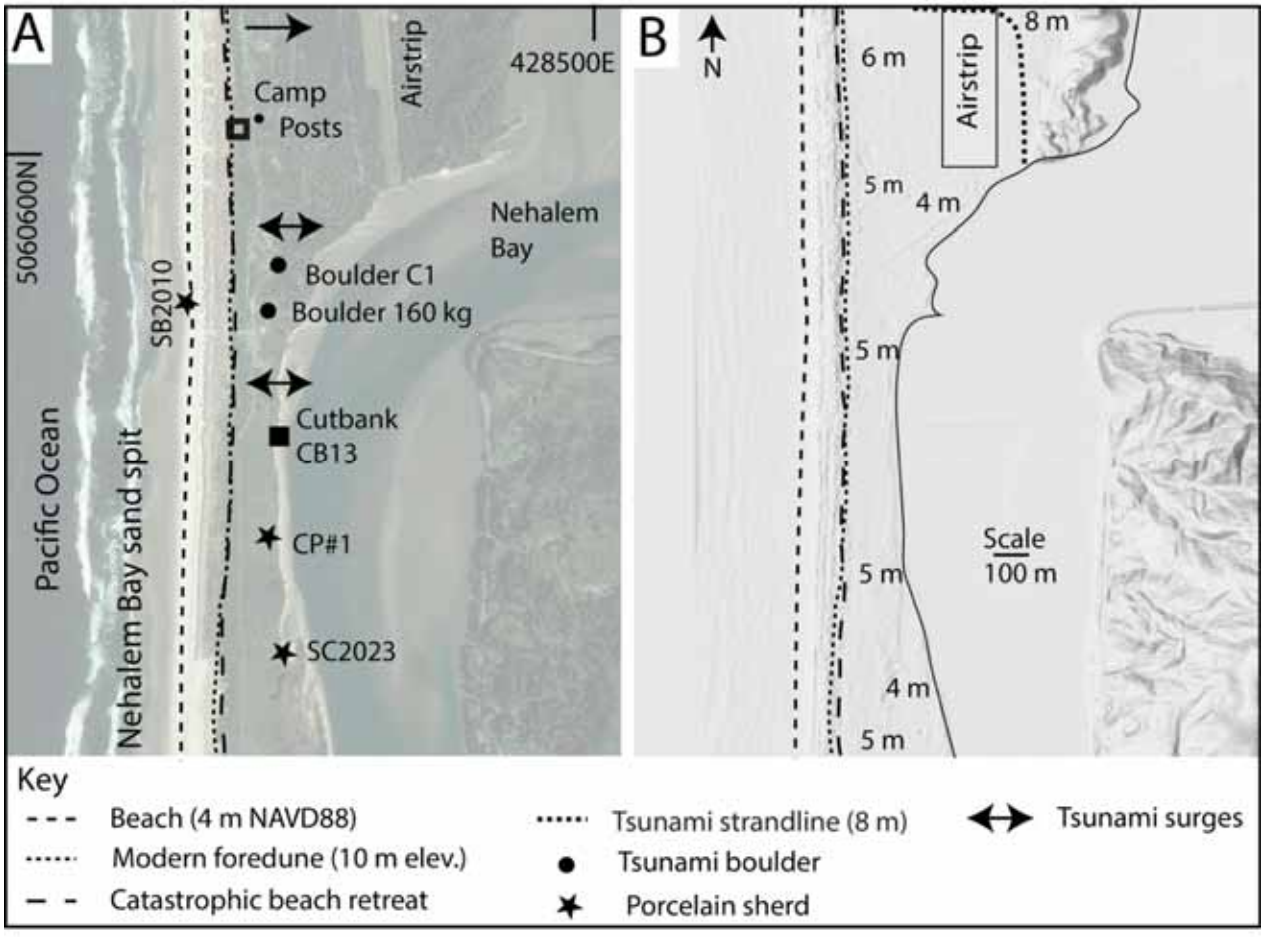

Figure 7. Satellite and hill shaded lidar images of the Nehalem Bay sand spit

Part A, satellite image including tsunami boulder sites (solid circles), cutbank site CB13 (solid square), and unabraded porcelain sherd sites (solid stars). The modern beach backshore (4 m NAVD88), modern foredune ridge (~10 m elevation), and catastrophic beach retreat scarp are plotted. Map coordinates are in meters UTM Easting and Northing. Part B, Lidar bare earth hill shaded image depicting dune features in the Nehalem Bay sand spit. Representative spot elevation data are in meters (m) NAVD88. Two small depressions or basins in the sand spit interior are represented by 4 m elevations.

As previously introduced in Peterson et al. (2011), the cutbank site CB13 (Figure 8) on the bay side of the central sand spit (Figure 7) demonstrates the sequences of tsunami surge scour, deposition, and dune burial in the central sand spit area. The CB13 cutbank demonstrates tsunami surge scour followed by beach-sand deposition (Figure 8). The initial tsunami surges were followed by surge backwash, which transported river sand and boulders (seaward) over the spit. Over the subsequent decades/centuries, remobilized tsunami sand and/or transgressive dunes (Figure 6) locally covered the tsunami deposits and associated Beeswax Wreck artifacts. In late historic time the dunes were stabilized by non-native invasive vegetation, including European dune grass (Oregon Historical Society, 2024) and now Scotch broom (Figure 7). The recorded tsunami surge sequences in the CB13 cutbank (Figure 8) account for the widespread Beeswax Wreck artifacts that have been collected across the interior of the sand spit and the Nehalem Bay wetlands (Williams et al., 2018). The initial landward-directed tsunami surge(s) could have remobilized previously beached Beeswax Wreck artifacts and transported them across the sand spit and into Nehalem Bay. Tsunami surges up the Nehalem Bay channel, from both overtopping of the sand spit and the propagation through the tidal inlet, could have further distributed the bayside artifacts, carrying some flotsam and sherd artifacts up the Nehalem Bay channel. Sites of shipwreck structures in the sand spit interior, including an upright hull section, dismembered timbers and a mast step, were reported to be in a sand covered basin, located ~0.5 km from the ocean beach (Rogers, 1899). Two such basins presently occur in the sand spit interior, as marked by 4 m elevations in Figure 7. It is not known whether Rogers (1899) was referring to the northern or southern sand covered basins in the central sand spit area. However, the northern basin is supported by later settler accounts (Giesecke, 2007).

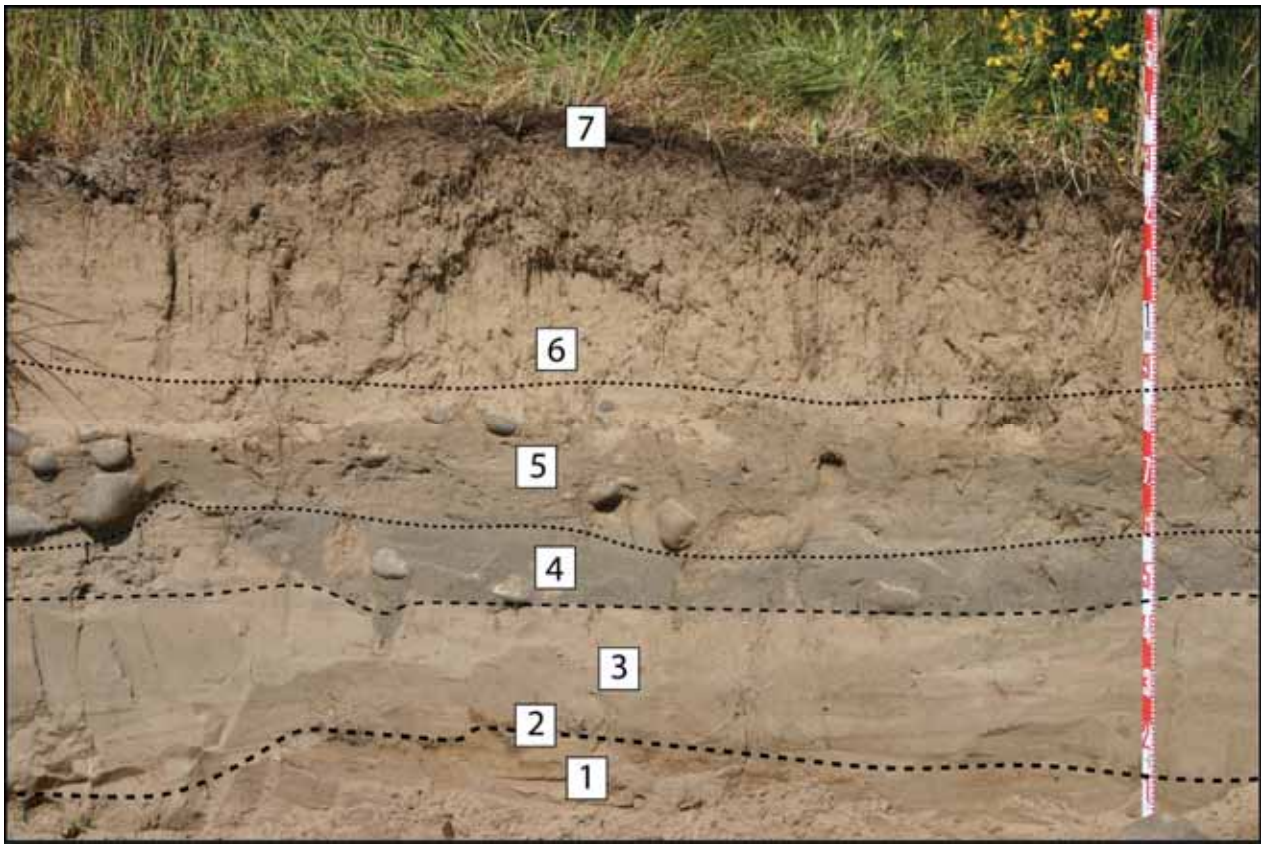

Figure 8. Cutbank exposure (CB 13) from the bayside shoreline of the Nehalem Bay sand spit

Photograph of the 1700 tsunami and cobble strata (cutbank site CB13) on the bayside shoreline of the Nehalem Bay sand spit (Peterson et al., 2011). Numbered stratigraphic events are (1) paleo-dune deposition, (2) basal truncation or scour by the 1700 tsunami surge (bold dashed line), (3) landward surge deposition of beach sand, (4) seaward surge deposition of river sand and gravel, (5) reversing surge deposition of beach sand, river sand, and cobbles, (6) historic dune transgression and localized or hummocky deposition, and (7) modern vegetative-stabilization of dune hummocks. See Figure 7 for cutbank site (CB13) location. Staff is color-marked in decimeter intervals.

Two large (6–7 cm wide) unabraded/uneroded or sharp-edged porcelain sherds including sherd CP#1 (Peterson et al., 2011) and sherd SC2023 (Figure 2B), were recently collected from the subaerially exposed 1700 tsunami cobble sheet, coeval with strata #5 in Figure 8, but as located further south on bay side of the central sand spit (Figure 7). The large sizes and unabraded conditions of both porcelain sherds suggest fragmentation and landward transport from a nearshore and/or beach source of shipwreck debris. The two sherds represent the southernmost bedload transported artifacts that are directly associated with 1700 tsunami surge deposits across the sand spit. They could point to a primary shipwreck site and associated breakup offshore or onshore of the central sand spit, prior to the alongshore dispersal of shipwreck structures and artifacts by wind, wave, and nearshore currents. The two unabraded porcelain sherd fragments are currently the only negatively buoyant artifact evidence, yet reported and archived, of a possible mid-spit shipwreck site. Precisely gridded high-resolution magnetic and metal detection surveys of the sand spit beach, foredunes, and swash zone for heavy iron artifacts, including cannons, anchors, and other large iron items, are warranted to better constrain a potential site of initial shipwreck breakup**.** By comparison, the Beeswax Wreck flotsam, including beeswax blocks and timber artifacts, were widely distributed along nearly the full length of Nehalem Bay sand spit, demonstrating along-shore dispersal prior to the 1700 tsunami surges. Such flotsam could have been locally concentrated at potential tsunami runup strandlines below the 8 m surface elevation contours at the north end of the sand spit (Figure 7).

In addition to the remobilization of shipwreck debris by tsunami surges there is evidence of widespread manual transport of the shipwreck cargo items, predominantly porcelain sherds, in Native American midden sites from the Nehalem area (Losey, 2002). Salvaging of porcelain sherds to make projectile points by Native Americans likely persisted for at least one century (1693 to early 1800s). So, the stratigraphic contexts of the manually remobilized porcelain sherds should post-date the 1700 emplacement of tsunami cobble sheets on the sand spit and/or the abrupt coseismic subsidence burial in the bay wetlands. Ongoing erosion of some tidal flat midden sites could be supplying manually remobilized porcelain sherds and/or debitage to the modern bayside beaches along the Nehalem Bay sand spit (John Dubè, pers. comm., 2024).

Lidar analyses of the south end of the Nehalem Bay sand spit (Figure 9) could support early historic settler claims of a shipwreck structure located at the south end of the Nehalem Bay sand spit (Rogers, 1899; Clarke, 1899; Williams, 2007). Two abandoned foredune ridges are shown landward of the modern foredune (Figure 9). The southernmost site of tsunami cobble recovery (C48) (Peterson et al., 2011) is shown at the northernmost extent of the pre-1700 foredune ridge. The northern portion of the pre-1700 foredune ridge is presumed to have been truncated or eroded by the 1700 tsunami surges. Catastrophic beach retreat is assumed to have shortly followed the 1700 coseismic subsidence, as approximated in Figure 9. The catastrophic beach retreat likely yielded a buried beach retreat scarp between the pre-1700 foredune and the historic foredune ridge. However, the presumed catastrophic beach retreat, following the 1700 coseismic subsidence, did not erode the remnant pre-1700 foredune ridge (Figure 10). So, a possible beached shipwreck structure trapped against the pre-1700 foredune ridge could have survived storm wave attack until eventual burial by historic beach progradation. Alternatively, a possible shipwreck structure that washed over the sand spit and into the Nehalem Bay channel could have been backwashed towards the tidal inlet and then lodged against the channel side of the pre-1700 foredune ridge (Figure 10).

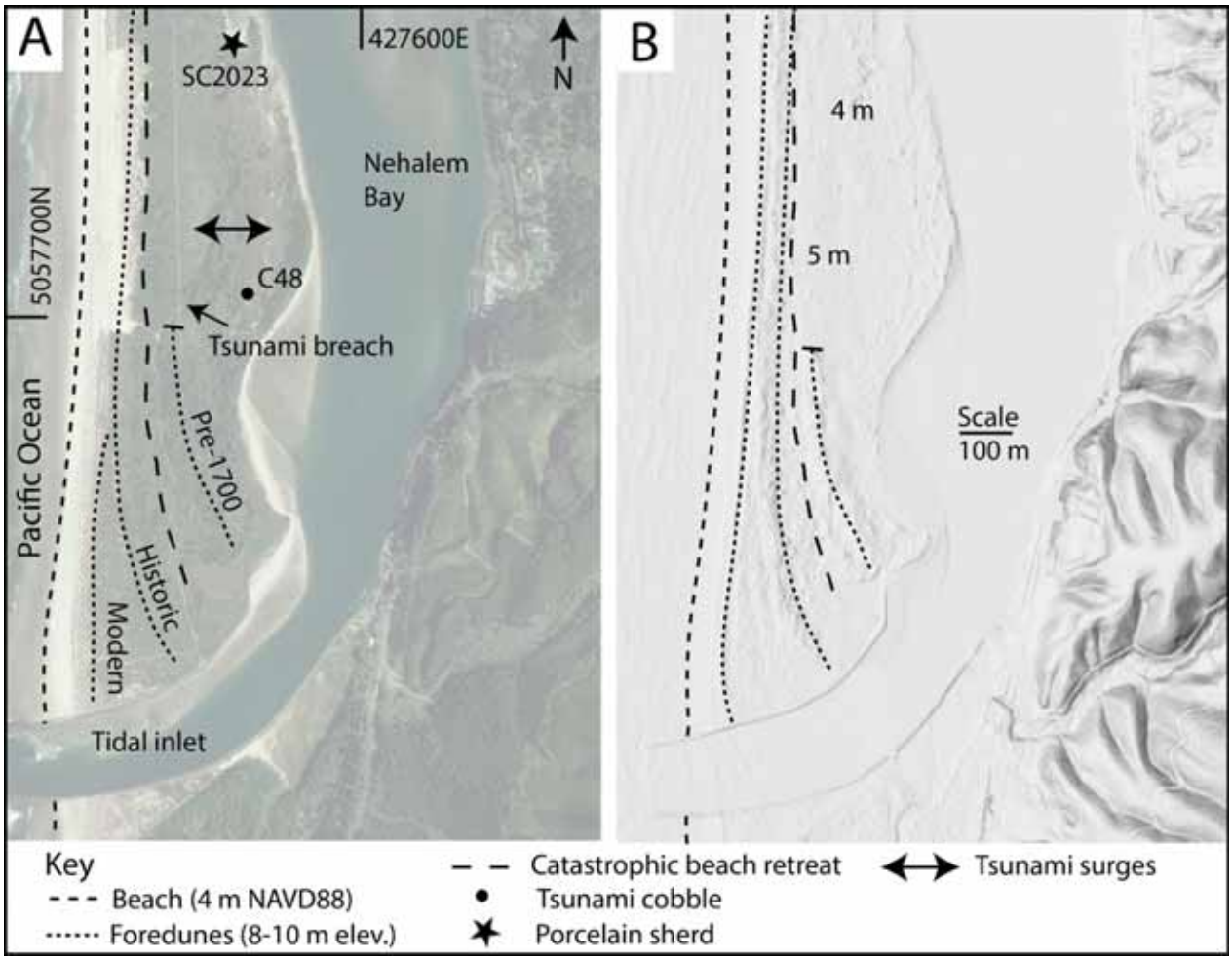

Figure 9. Satellite and hill shaded lidar images of the south end of the Nehalem Bay sand spit

Part A, satellite image of the south end of the Nehalem Bay sand spit and Part B, lidar image including the modern beach backshore (short, dashed line), abandoned foredune ridges (dotted lines), and the catastrophic beach retreat scarp. The beach retreat scarp is mapped at ~150 m east of the modern backshore, and between the pre-1700 foredune and the historic foredune in the southernmost part of the sand spit.

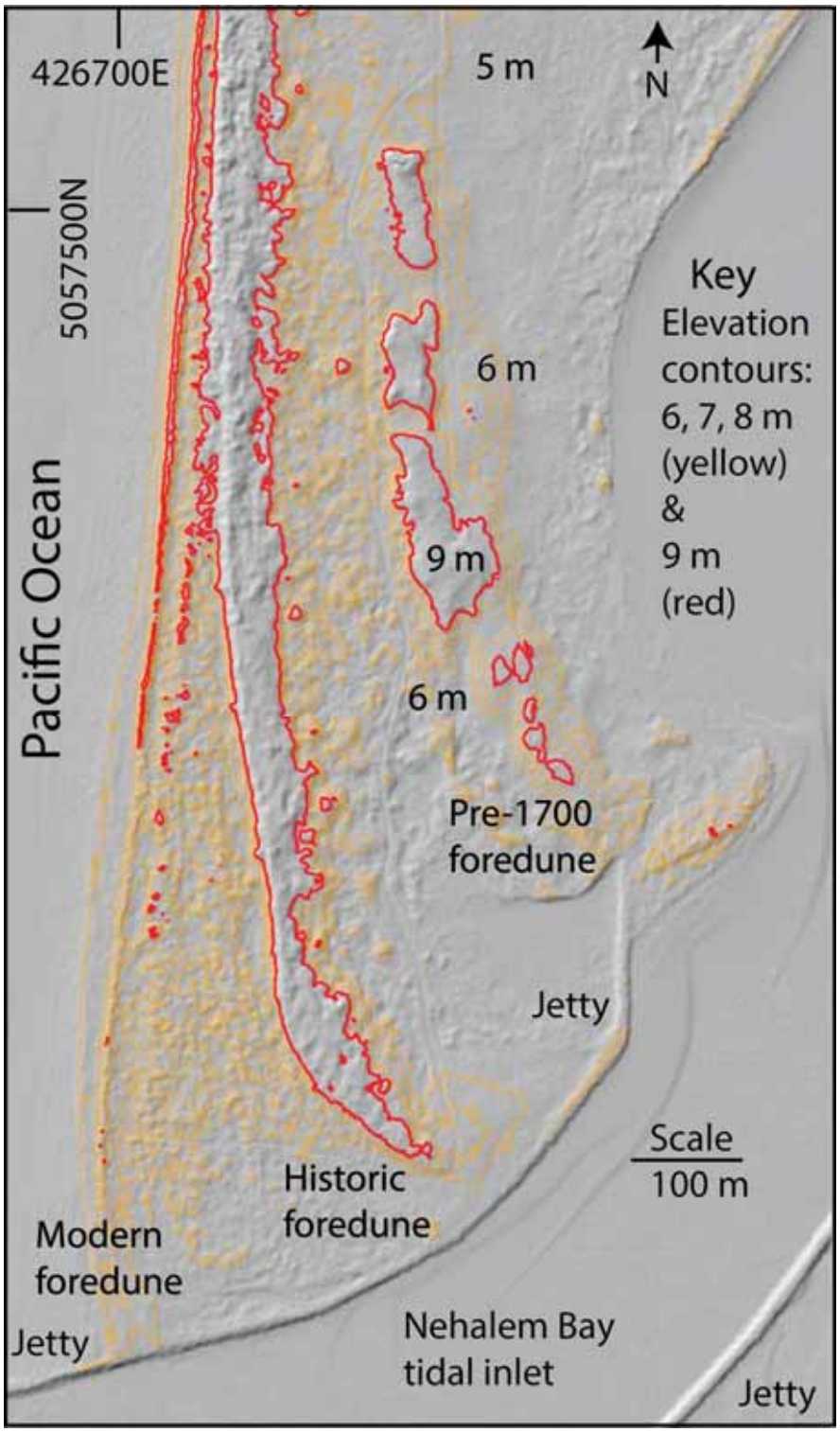

Figure 10. Contoured lidar elevation map of the south end of Nehalem Bay sand spit

Elevation contours outline abandoned foredune ridges at the southern end of the Nehalem Bay sand spit. The southernmost end of the pre-1700 foredune ridge locally survived the 1700 tsunami surges but was truncated to the north by the tsunami surges. The remnant pre-1700 foredune ridge (9 m elevation) could host a tsunami remobilized shipwreck structure on its seaward side. Alternatively, tsunami backwash could have transported shipwreck debris towards the tidal inlet with localized lodgment of some debris against the bayside of the pre-1700

foredune ridge. Either locality could correspond to historic accounts of a shipwreck structure located at the south end of the sand spit (Rogers, 1899; Clarke, 1899).

4.3 1700 Tsunami Runup Records in Elevated Wetlands

Two elevated wetland settings were examined for maximum recorded runup records of the 1700 tsunami surges in the study area. One setting is a proximal ocean shoreline locality at the Doris Hassler Davis Pond wetlands (Figure 2C). The other setting is a proximal estuary shoreline locality at the Manzanita Bayside wetlands. Maximum recorded 1700 tsunami surge runups are based on tsunami sand layers and associated tsunami sandy-debris caps (Table 2), as recorded in gouge core transects (Figure 11 and Figure 12). Historic records (1915) of abundant beeswax in the Neahkahnie marsh (Cooper Borge, 1975) date the shallow, anomalous beach sand layer in the Doris Hassler Davis Pond wetlands to the 1700 tsunami surge(s). There are no historic storm surge deposits above the 1700 tsunami sand layer in the Doris Hassler Davis Pond wetlands (Figure 11). The youngest abrupt coseismic subsidence and tsunami sand horizon at the Manzanita Bayside shoreline (core site BG1) is correlated to the C^{14}-dated 1700 coseismic subsidence horizon in a nearby reconnaissance core site (Grant, 1994). The measured burial depths of the tsunami sand layer at the subsidence contacts diminish from 0.6 m to only 0.4 m in the supratidal wetland settings (Figure 12) due to their elevations above the high tide levels (Table 1). No river flood or eolian sand layers are evident above the 1700 subsidence contact in core site BG1 (Figure 12B). The late historic 1964 and 1996 Nehalem River floods (100-year flood levels) left no apparent sandy deposit records in the peaty deposits of the Manzanita Bayside wetlands.

Table 2. Runup elevation data from 1700 tsunami deposits in proximal shoreline wetlands

Locality/Core Site	UTM E (m)	UTM N (m)	Site Elevation (m NAVD88)	Tsunami Detritus Depth (cm)	Tsunami runup (m NAVD88)
Doris Davis					
DD1	426790	5064100	7.6	30-32	7.3
DD2	426850	5064110	8.2	21-23	8.0
DD3	426870	5064100	8.5	19-26	8.2
DD4	426910	5064080	9.1	25-32	8.8
DD5	426940	5064070	9.7	37-41	9.3
DD6	426970	5064080	10.0	-	-
DD7	426990	5064090	10.1	-	-
Bayside Gardens					
BG1	428690	5062020	3.1	57	2.5
BG2	428710	506060	3.6	28-34.5	3.3
BG3	428680	5062090	3.8	26-29	3.5
BG4	428690	5062110	4.2	-	-
BG5	428690	5062160	4.5	-	-

Table 2. Core sites (DD) are from the Doris Hassler Davis Pond wetlands. Core sites BG are from the Manzanita Bayside (Gardens) wetlands. See Figure 1C for core localities and Figure 10 and Figure 11 for core site positions in meters (m) UTM easting (E) and Northing (N). Core site lidar elevations in meters (m NAVD88) are reported to 0.1 m resolution (DOGAMI 2024), but close spaced lidar targets in the wetlands varied by as much as ±0.2 m elevation.

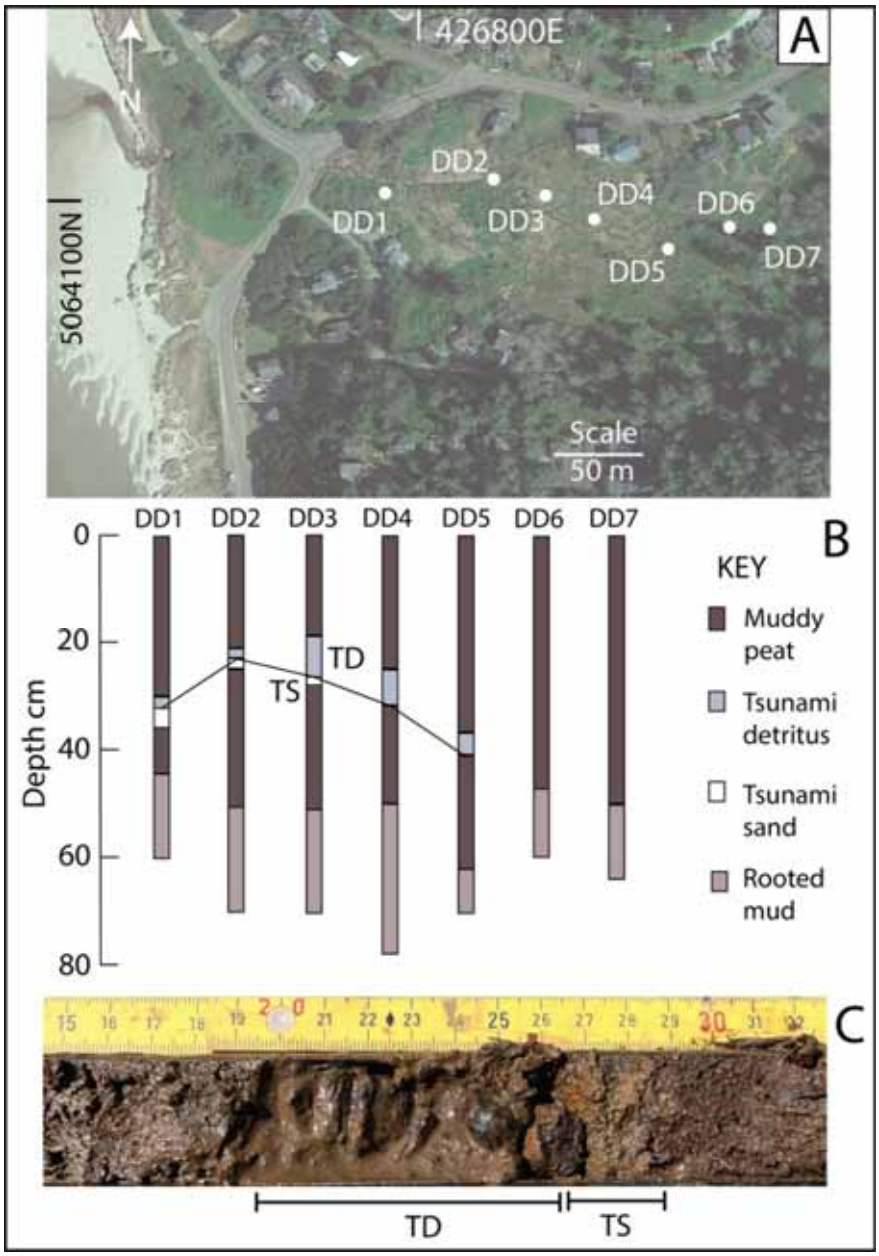

Figure 11. Site map and core logs of 1700 tsunami deposits in the Doris Hassler Davis Pond wetlands

Part A, core site positions in the Doris Hassler Davis Pond wetlands. See Table 2 for core site coordinates and elevations, and Figure 1C for Doris Hassler Davis Pond location. Part B, core logs from the Doris Hassler Davis Pond wetlands. Part C, photograph of core DD3 showing tsunami sand layer (TS) and overlying tsunami sandy detritus layer (TD). Rounded quartz-rich sand grains (beach source) in the tsunami sand deposits are differentiated from potential angular lithic-rich sand grains (creek source) from the Neahkahnie Mountain (basalt) tributaries (Niem and Niem, 1985).

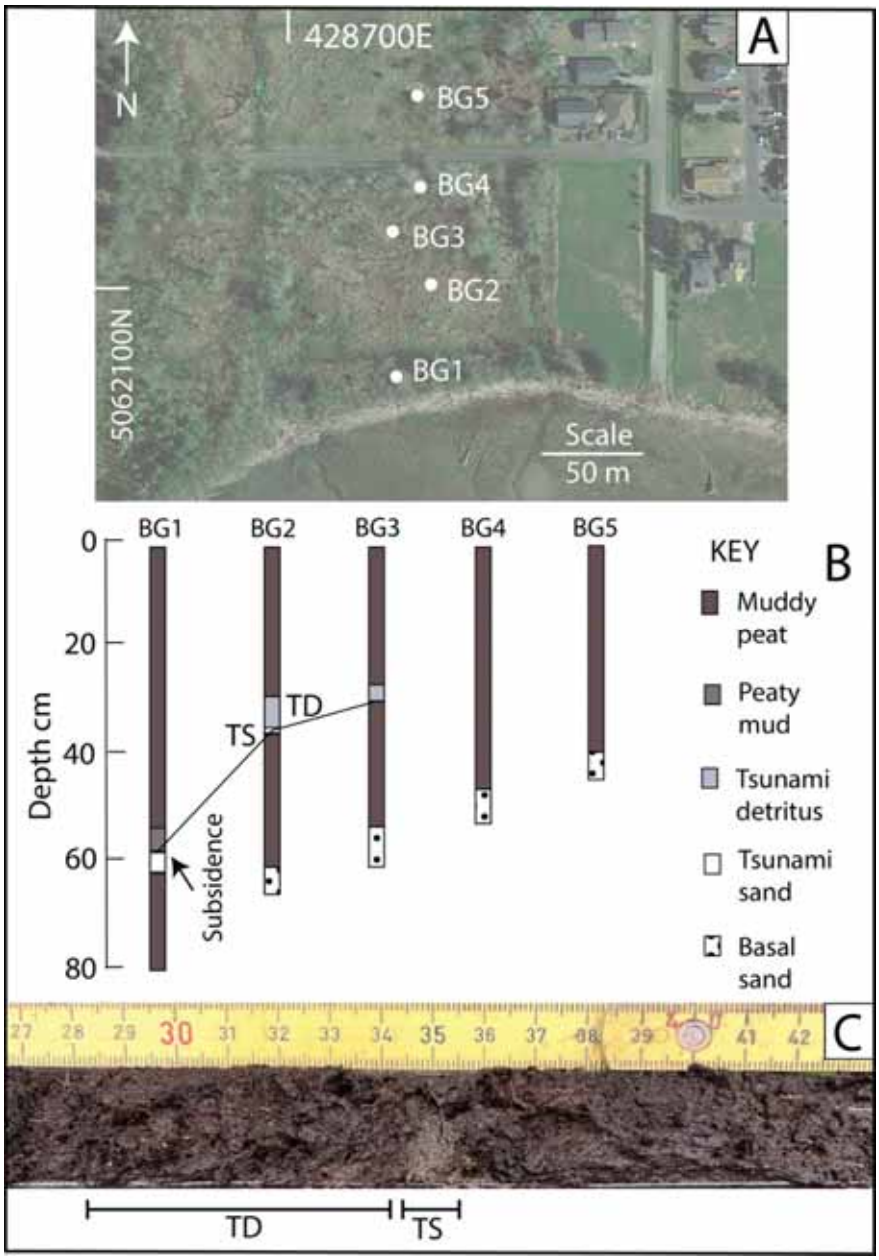

Figure 12. Site map and core logs of 1700 tsunami deposits in the Manzanita Bayside wetlands

Part A, core site positions in the Manzanita Bayside wetlands. See Table 2 for site coordinates and elevations and Figure 1C for Bayside wetland location. Part B, core logs from the Manzanita Bayside wetlands. Part C, photograph of core BG2 showing thin tsunami sand layer (TS) and overlying tsunami sandy detritus layer (TD). Subangular lithic-rich sand grains (river/bay source) in the Manzanita Bayside tsunami deposits are differentiated from potential rounded quartz-rich sand grains (eolian source) from the nearby Manzanita dune field.

The maximum elevation of the sandy organic detritus layer at the Doris Hassler Davis Pond wetlands (site DD5) is 9.3 m elevation NAVD88 (Table 2). The ~8.0 m elevation values for the tsunami sand layers at DD2 and DD3 (Figure 11) agree with 7.5–8.0 m tsunami sand layer elevations for the 1700 tsunami surges at nearby Cape Lookout (Figure 1B) (Minor and Peterson, 2016). The maximum elevation reached by tsunami sandy organic detritus layers at the Manzanita Bayside wetlands is 3.5 m elevation (Figure 12). Surprisingly, the terminal tsunami detrital layer in the Manzanita Bayside wetlands (site BG3 in Figure 12) is 1.5 m lower in elevation than the entrained tsunami boulder (C1) at 5 m elevation in the interior of the northern Nehalem Bay sand spit (Figure 7). The relatively higher backwash flow over the sand spit, relative to the Bayside wetlands, might reflect

momentum-enhanced runup over the sand spit where the main channel backwash flow was directed against the sand spit.

The tsunami sandy detritus layers in the Doris Hassler Davis Pond wetlands and Manzanita Bayside wetlands contain sand grains that had adhered to the tsunami flow-suspended woody/leaf litter organics. The most landward sandy detritus layers likely reflect waning flow velocities and shallowing water column depths that occurred prior to landward surge termination. The maximum landward extents of the recorded tsunami detritus layers in the two wetland transects are assumed to represent maximum tsunami surge runups, respectively, in the ocean beach and estuary wetland settings. Whereas the proximal ocean setting received the full open-ocean tsunami impact, the distal inshore wetland tsunami impacts were dampened by surge dissipation over the broad tidal flats. The measured tsunami runup values are used to predict widely distributed 1700 tsunami strandlines and the potentials for associated Beeswax Wreck flotsam transport in the Manzanita beaches and in the Nehalem Bay wetlands and upper bay floodplain, as presented later in this article.

4.4 Manzanita Beach Retreat Features and the 1700 Tsunami Strandline

Catastrophic retreat or erosion of the ocean beaches fronting the Manzanita dune field and the Nehalem Bay sand spit (Figure 1C) followed the 1700 tsunami surge runups, due to coseismic coastal subsidence (Figure 3) (Peterson et al., 2011). The catastrophic beach retreat persisted for about two centuries (Figure 13A) until the combination of interseismic uplift, estuary infilling, and river sand bypassing to the study area beaches, initiated beach seaward progradation (Figure 13B). The initial catastrophic beach retreat resulted from a displacement of beach sand to the innermost shelf (10–30 m water depth), where it filled the post-subsidence offshore accommodation space (Brunn, 1962; Brunn, 1988; Peterson et al., 2020). At least two centuries of interseismic uplift since the 1700 megathrust rupture (Cruikshank & Peterson, 2017) likely reduced the post-subsidence sand burial depth to ≤0.50 across the innermost shelf in late historic time. River sand supply to the study area beaches, possibly enhanced by extensive logging in the study region drainage basins, likely contributed to the onset of beach progradation in late historic time. The retreat cobble berms, still exposed in early historic time (Figure 13A), would have been observed as stone seawalls to early settlers salvaging shipwreck timbers along the ocean beaches (Figure 4 and Figure 6). Relations between the estimated tsunami runup strandlines, catastrophic beach retreat, beach recovery by seaward progradation, and subsequent burial by transgressive dune sand are quantified in across-shore borehole transects (2023) taken along previously occupied GPR lines (2007–2008), as presented below.

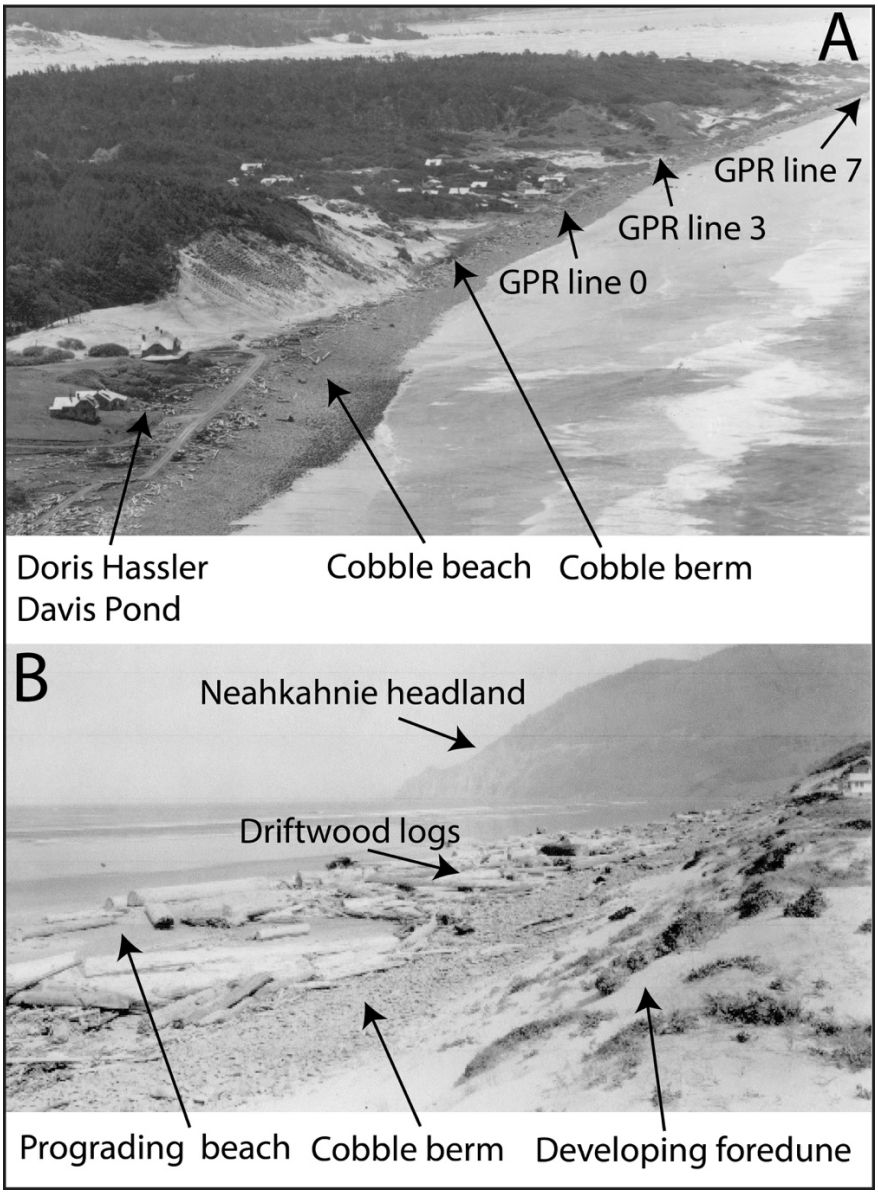

Figure 13. Historic photographs of the Manzanita beaches

Part A, historic oblique aerial photograph (circa early 1920s) of exposed beach cobble and beach retreat cobble berm in the Manzanita beaches. View is to the south. Note the contrast between the severe shoreline erosion of the Manzanita beaches in the 1920s and the broad modern beaches in Figure 4A. See Figure 4B for the mapped locations of GPR/auger borehole transect lines 0, 3, and 7. Part B, historic photograph (circa 1930s–1940s) showing onsets of 1) sandy beach progradation, 2) burial of cobble berm, and 3) incipient foredune development. The accumulation of driftwood logs is apparent in the beach backshore located north of GPR line 0. View is to the north. Historic photographs were discovered by one of these authors (Mock) in the archives of the Nehalem Valley Historical Society Museum, Manzanita, Oregon.

Across-shore GPR lines and associated sand auger borehole transects establish the positions and elevations of 1) dune ramp paleosols that were inundated by the 1700 tsunami runup surges (9 m NAVD88), 2) post-1700 subsidence catastrophic beach retreat scarps and beach retreat cobble berms, 3) late historic beach progradation, and 4) burial of prograde shorelines by transgressive dunes and vegetatively stabilized foredunes (Figure 14). During initial ground truthing of the GPR profiles by borehole auguring (Peterson and Cruikshank, 2007) buried stone features were found to be associated with the catastrophic beach retreat scarps. But it was not known what or who had built the buried stone features at the backshores of the broad sandy beaches. Recent discovery (2023) of archived historical photographs of the Manzanita beaches were followed by additional borehole auguring (2023), which identified the buried stone features as beach retreat cobble berms (Figure 13). The measured distances

between the modern beach backshore settings at 4 m elevation (NAVD88) and the same elevation in the catastrophic beach retreat scarps, as imaged in GPR lines 0–7 (Figure 14), average 140 m. In this article a conservative distance of 130 m landward of the modern beach backshore (4.0 m elevation by lidar) is used to map the alongshore position of the catastrophic beach retreat scarps in Figure 4 and Figure 7. Due to jetty enhanced beach progradation at the south end of the Nehalem Bay sand spit (Figure 9) a greater distance (~150 m) is used to predict the position of catastrophic beach retreat scarp in that location.

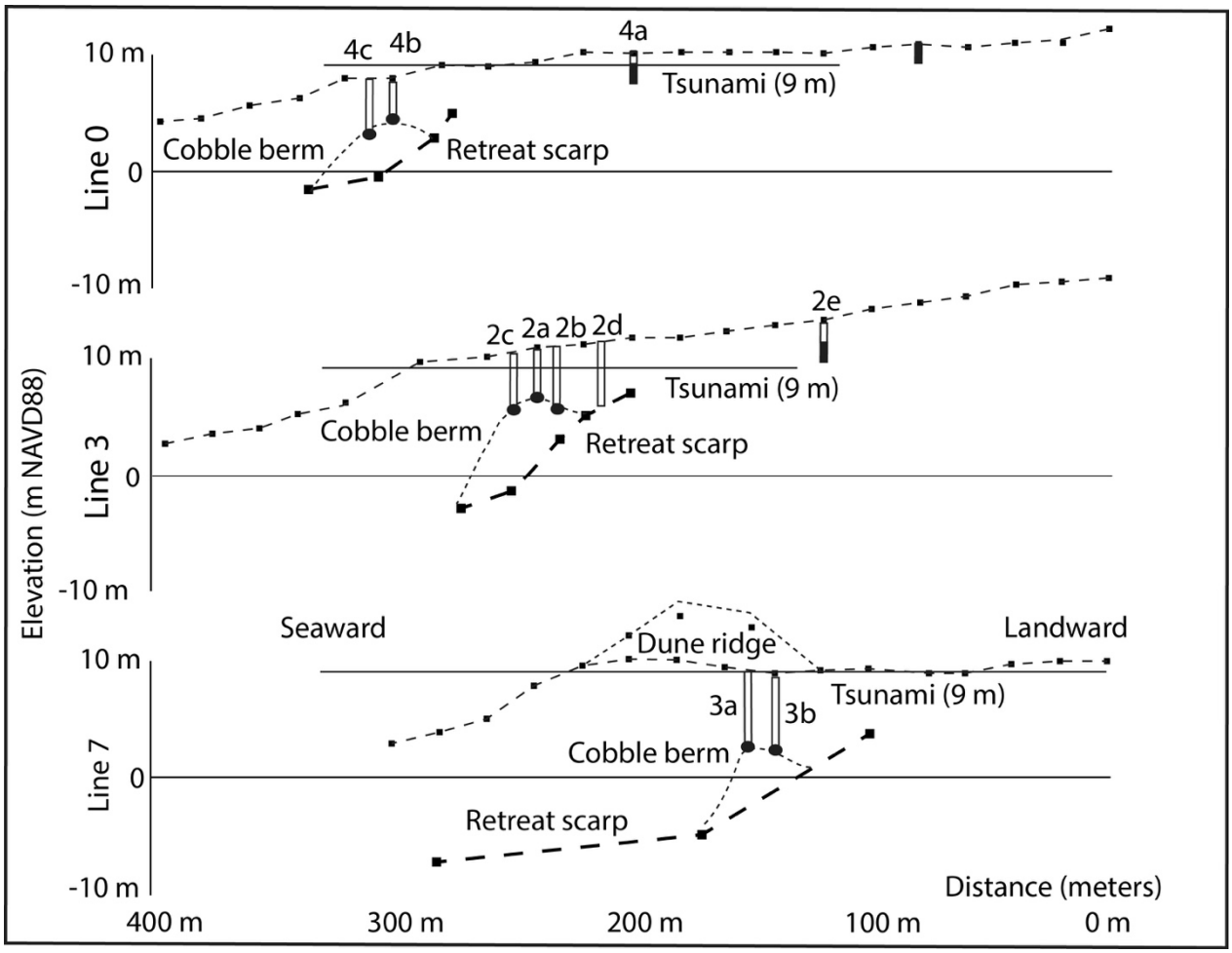

Figure 14. Cross-sections of GPR line and borehole transects in the Manzanita beaches

Cross-sections of selected GPR/auger borehole profiles (lines numbered 0, 3, 7), include 1) surface topography (relative to 0 m NAVD88), 2) sand auger boreholes (numbered columns), 3) contacts with beach retreat cobble berms (solid ellipses), and 4) catastrophic beach retreat scarps (bold dashed lines). GPR profiling was completed in 2007–2008 (Peterson and Cruikshank, 2007; Peterson et al., 2011). Borehole transects were completed in 2023 to establish the topography of the buried retreat cobble berms. Dune paleosols with soil Bw horizons (black columns) are shown for GPR/ auger borehole lines 0 and 3, as completed in 2023. Estimated tsunami maximum runup is shown at 9 m elevation (horizontal line), as taken from Figure 11. Locations of the GPR/borehole transect lines are shown in Figure 4 and Figure 13A.

Stripped lower-deck structures might have existed on the ocean beaches after the 1700 tsunami remobilization(s), but they would have been further dismembered by catastrophic beach erosion that followed the 1700 coseismic subsidence (sequence 2 in Figure 15). Ballasted shipwreck keel/bilge structures and large metal artifacts in the nearshore zone would have been eroded down to the wave-scoured surf zone base levels and/or dispersed alongshore or offshore by decades of winter wave attack. Sherds, small water-logged wooden artifacts, and/or other negatively-buoyant materials that were transported offshore to the innermost-shelf (10–30 m water depth) would have been buried by offshore accommodation space filling, following the coseismic subsidence of ~1.0 m (Nelson et al., 2020) and prolonged sea level rise (Figure 3) (Peterson et al., 2020). Interseismic uplift probably reduced the burial depth to ≤0.5 m during late historic time (Cruikshank and Peterson, 2017) when the displaced

beach sand returned to the study area beaches (Figure 13B). Shallow burial depth(s) of small artifacts across the innermost shelf would have permitted remobilization of some buried artifacts by winter storm wave scouring. However, any ballasted timber structures and/or large metal artifacts that survived winter storm wave attack on the exposed or retreat eroded beach platforms would have been eventually buried by beach progradation (sequence 3 in Figure 15). Such progradation would have buried the surviving shipwreck artifacts by as much as 5 m of beach sand. Subsequent dune transgression and/or stabilized foredune development would have further buried the beached artifacts to total depths of 5–10 m subsurface (sequence 4 in Figure 15). Future beach sand loss from predicted global sea level rise (Peterson et al., 2020) could release some of the buried shoreline artifacts back to active transport during the next century.

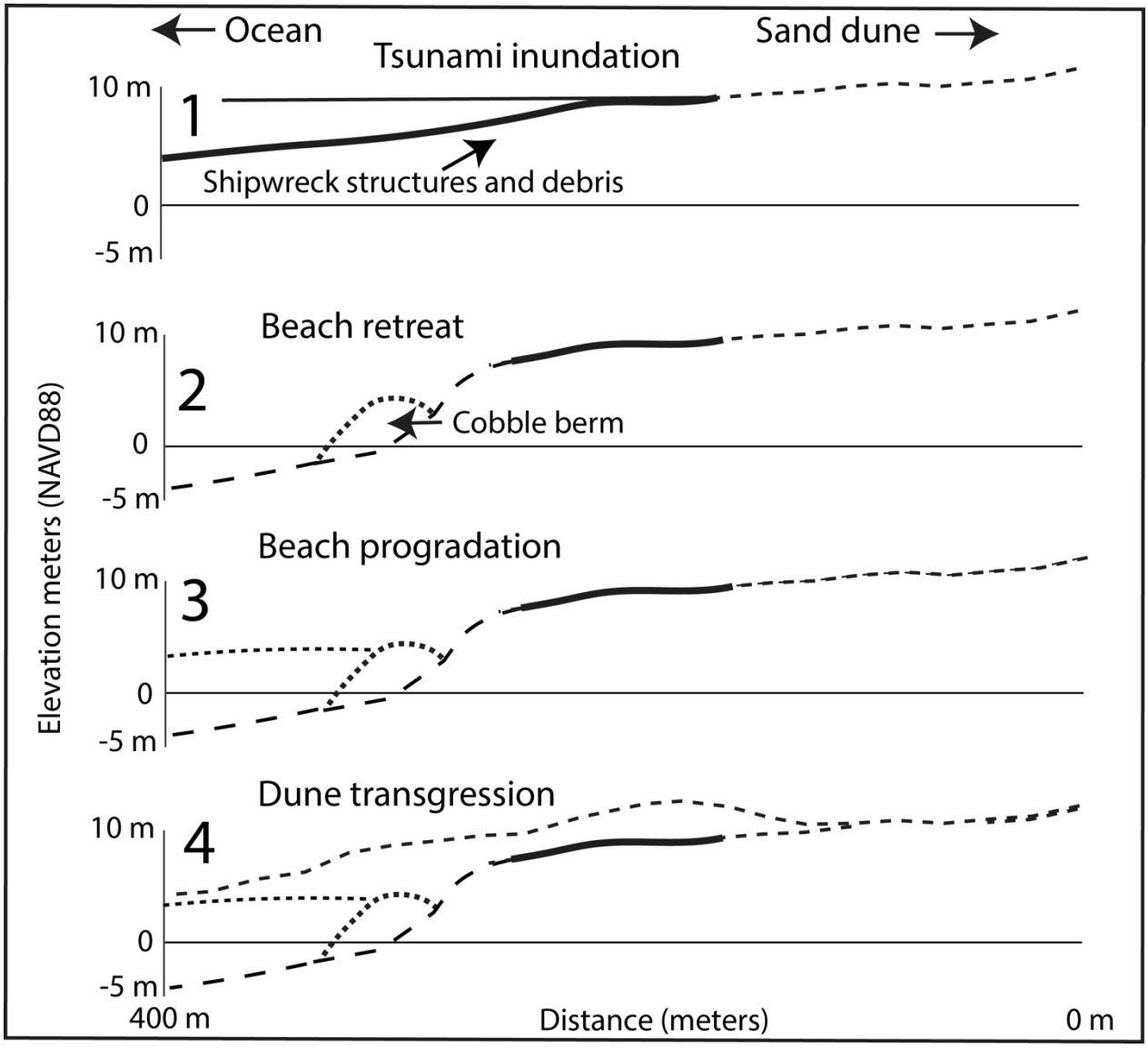

Figure 15. Diagram of tsunami inundation, beach retreat, progradation, and dune burial of study area ocean beaches

Representative sequences of 1700 tsunami inundation, catastrophic beach erosion, and remaining artifact burial by subsequent beach progradation and dune burial. These generalized sequences are based on GPR line/borehole transects in the Manzanita beaches and Nehalem Bay sand spit. Sequence 1 is the 1700 tsunami inundation (bold line) and associated landward remobilization of shipwreck structures and smaller debris. Sequence 2 is the catastrophic beach retreat and associated development of a beach retreat cobble berm from coseismic subsidence. Sequence 3 is the beach recovery and shoreline progradation from interseismic uplift. Sequence 4 is the historic dune burial and preservation of shipwreck artifacts.

In contrast to possible beached lower-deck structures and large metal artifacts, the smaller disjointed structures and flotsam artifacts from the Beeswax Wreck could have been transported by tsunami surges to positions located landward of the beach retreat scarps. Those artifacts would have been preserved from winter storm-wave attack (sequence 2 in Figure 15). Beeswax Wreck flotsam artifacts that are preserved between the catastrophic beach erosion scarps and the 1700 tsunami maximum runup elevations are now buried by transgressive dune cover and/or by stabilized foredunes (sequence 4 in Figure 15) to depth of 5–10 m subsurface (GPR lines 3 and 7 in Figure 14). The Nehalem Bay sand spit areas (GPR Lines 1 and 7) lack dune ramp paleosols landward of their beach retreat scarps. Given the expected elevations of pre-1700 tsunami beach backshores and incipient foredune surfaces (5–6 m NAVD88) along the Nehalem Bay sand spit (Figure 7), some small shipwreck structures could have been remobilized by the tsunami surges to positions located 1) landward of the subsequent beach retreat scarps (Figure 6), or 2) entirely across the sand spit to the Nehalem Bay channel. Tsunami backwash surges could have remobilized stranded shipwreck debris on the lower elevations of the sand spit or even have transported shipwreck debris back across the spit to the ocean beaches.

4.5 Beeswax Artifact Recovery from Nehalem Bay Wetlands and Floodplains

Beeswax blocks have been collected and reported from 1700 tsunami runup sites on the Nehalem Bay sand spit, along the banks of Nehalem River channel, and in adjacent fluvial-tidal floodplains (Figure 16A) (Williams et al., 2018). Cold ocean water in the study region precludes the formation of typhoons or hurricanes and their potentially large storm surges (Pittock, 1982). Only catastrophic nearfield tsunami inundation could both reverse the fluvial-ebb tidal flow in the upper bay channels and overtop the fluvial-tidal floodplains in the upper bay reaches. During the 1700 megathrust rupture, coastal coseismic subsidence of ~1.0 m (Nelson et al., 2020) resulted in prolonged sea level rise in the study region (Figure 3). Interseismic uplift over the next couple of centuries largely retuned the coastal land levels to their pre-1700 elevations, but net sedimentation buried the pre-1700 wetland surfaces and associated tsunami deposited shipwreck flotsam artifacts by 0.3–0.6 m of mud and peat (Figure 12B). The possible extents of tsunami sand deposits in the uppermost reaches of Nehalem Bay are not known. Such potential tsunami sand laminae might be difficult to discriminate from river flood deposits in the fluvial-tidal floodplains. In this article, the reported positions of collected beeswax blocks, as excavated from shallow (≤1 m depth) drainage ditches or stump removal cavities in dairy pastures, are used as proxies for tsunami surge inundations or strandlines in the upper reaches of Nehalem Bay. Most recently, one such beeswax block came to be reported (2024) from near the head of tide in the North Nehalem River floodplain (NF3 in Figure 16A). These authors visited the site of the recovered beeswax block (Figure 16B) and measured the 1700 subsidence contact at 0.6 m depth below the modern floodplain surface (2.9 m NAVD88), yielding a tsunami-inundated surface of 2.3 m elevation. Assuming a flow depth of at least 0.4 m to float the large beeswax block, the NF3 site data would translate to a tsunami runup elevation of 2.7 m NAVD88 at the NF3 site, located ~14 km upriver of the Nehalem Bay tidal inlet (Figure 16A).

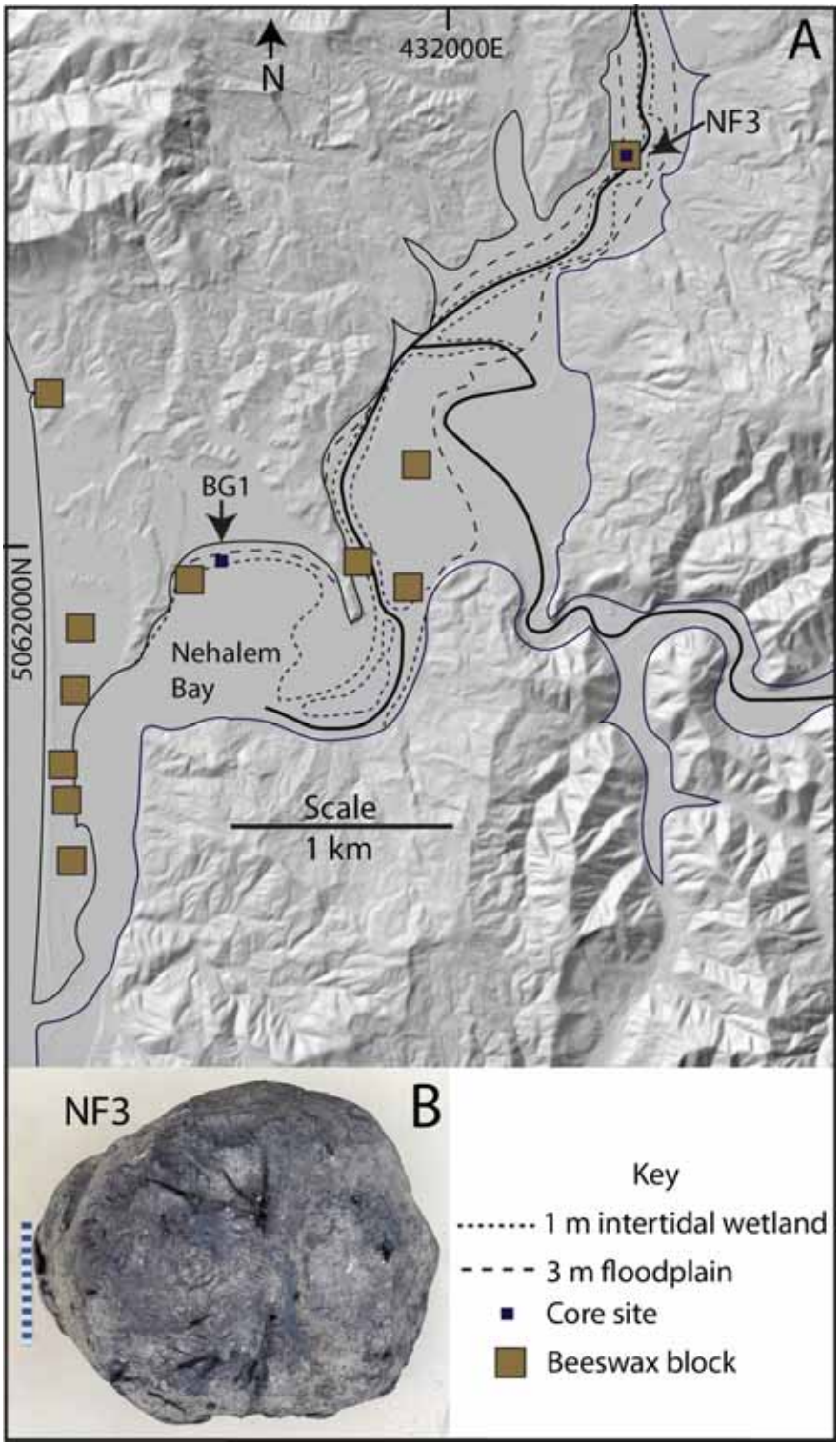

Figure 16. Lidar map of beeswax block artifacts collected in the Nehalem Bay wetlands

Part A, locality map of recovered beeswax blocks (brown boxes) (Williams, 2018). See Figure 12B for the core log from site BG1 in the Manzanita Bayside wetlands. Tidal marsh is mapped at ≥1 m elevation (dotted line) and supratidal floodplain is mapped at ≥3 m elevation (dashed line). Intervening vegetated wetlands and fluvial-tidal floodplain (2.0±1.0 m) could host tsunami transported flotsam artifacts. Lidar bare earth hill shaded base map is from DOGAMI (2024). Part B, a recently reported (2024) beeswax block (27 kg) was collected from the North

Fork Nehalem River fluvial-tidal floodplain (site NF3 in Part A). Scale (vertical, photo left) is 20 cm in total length.

5. Discussion

5.1 Pre-1700 Tsunami Beeswax Wreck Artifact Dispersal

Specifics about the position and timing of the Beeswax Wreck grounding and breakup are not known directly. However, the net directions and averaged rates of artifact dispersals provide constraints on these unknowns. Beeswax Wreck timbers were preserved under the 1700 rockslide boulders on the intertidal platform in the north side of Smuggler Cove (Figure 1C) (Peterson, et al., 2023). Beeswax blocks were historically reported from the Doris Hassler Davis Pond wetland (Figure 11) (Cooper Borge, 1975). No porcelain sherds were observed in the 1930s by Paul See in the 'teak' timber tsunami runup deposits along the Manzanita beaches (Figure 4) (Paul See, pers. comm., 2008). Porcelain sherds have been observed in association with 1700 tsunami cobble layers in the central part of the Nehalem Bay sand spit (Figure 7). Beeswax Wreck sherds have also been collected along beaches on the northern bayside shoreline of the Nehalem Bay sand spit (Lally, 2008; Lally, 2016; Litzenberg, 2022). But no sherds have been identified in the initial landward surge strata or overlying tsunami gravel deposits in the north spit area (John Dubè, pers. comm., 2024). Therefore, it is not known whether the sherds in the northern spit bayside beaches were derived from 1) landward surges overtopping the northern spit area, 2) secondary surges propagating up the Nehalem Bay channel, and/or 3) post-tsunami manual transport. No sherds are reported from modern beaches or paleo-foredune ridges located south of the Nehalem Bay sand spit. Beeswax blocks are rarely reported from pre-1700 foredune ridges, barraged lagoons, and/or the Tillamook Bay tidelands located south of the Nehalem Bay sand spit (Figure 1B). The Nehalem Bay tidal inlet is too small to significantly block southward transport of flotsam. So, the relative paucity of recovered beeswax and shipwreck timbers from south of the Nehalem Bay tidal inlet suggests a dominant northward dispersal of shipwreck flotsam from a shipwreck site, or sites, located north of the Nehalem Bay tidal inlet. In historic time, driftwood logs from the Nehalem and Tillamook drainages accumulated at the north end of the Manzanita beaches (Figure 13B), demonstrating northward transport of driftwood in the study area during recent time. For this article we take the separation distances between the two large unabraded sherds (SC2023 and CP#1) (Figure 17A) as a minimum dispersal distance (northward) for bedload transported sherds, prior to the 1700 tsunami inundations. Similarly, the separation distances between sherd SC2023 and the Doris Hassler Davis Pond site of tsunami remobilized and deposited beeswax blocks is taken to be the minimum dispersal distance of beeswax blocks, prior to the 1700 tsunami inundations. The separation distances between sherd SC2023 and the North Smuggler Cove site of 1700 coseismic rockslide burial of Beeswax timbers is taken to be the minimum dispersal distance of the shipwreck timbers, prior to the 1700 great earthquake coseismic shaking.

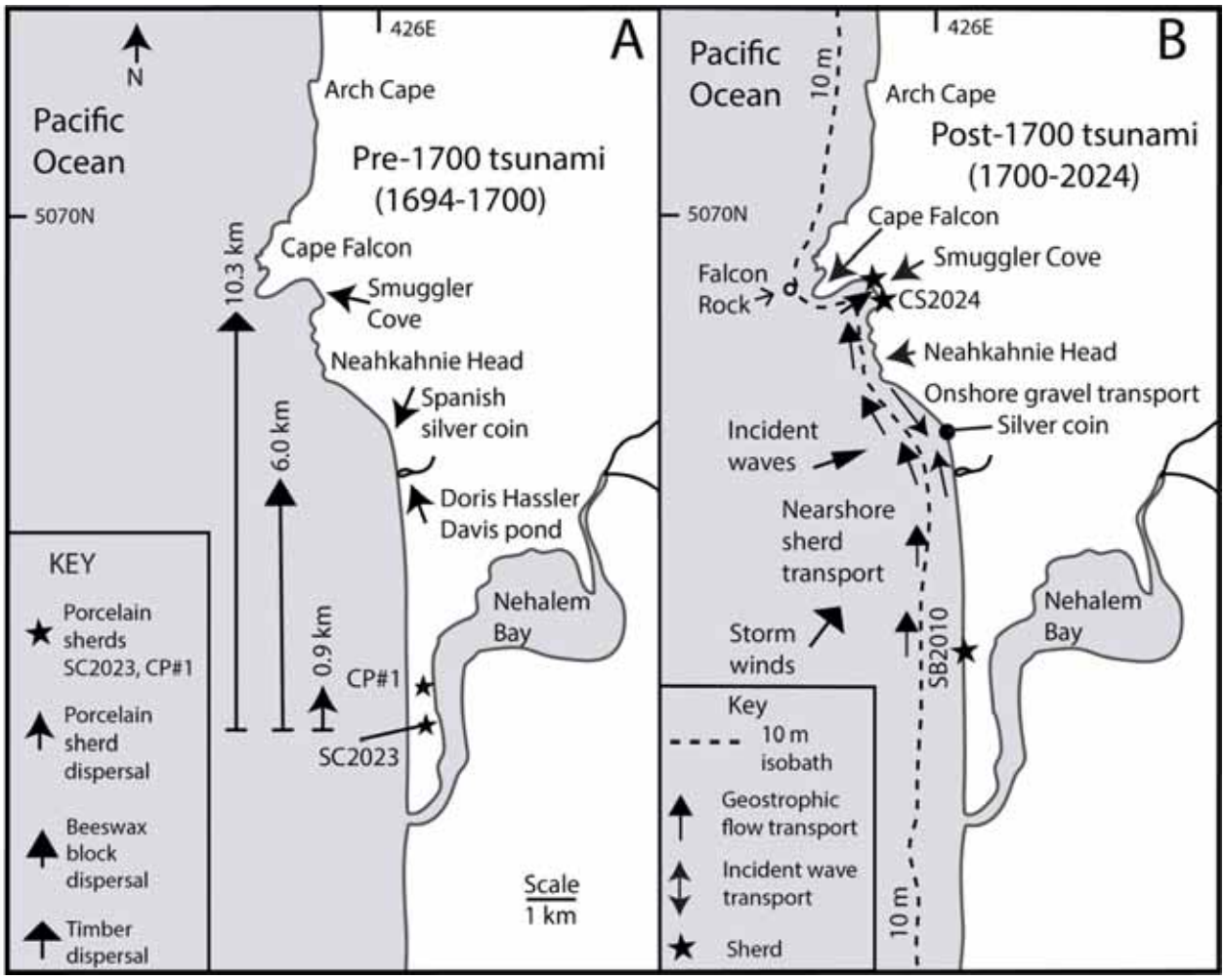

Figure 17. Maps of Beeswax Wreck artifact dispersals in the study area

Part A, map of measured Beeswax Wreck artifact dispersals prior to 1700 tsunami inundations. Northward alongshore distances are measured from the site of the southernmost unabraded porcelain sherd (SC2023) (Figure 7). Artifact dispersal localities are based on artifact association with 1700 tsunami deposits or 1700 rockslide burials. Part B, map of directional transport with catchment topographies/bathymetries and sites of 1) Spanish coin (Figure 18D) collected at a storm cobble berm, located south of Neahkahnie Head, 2) slightly abraded porcelain sherd SB2010 (Figure 18B) collected from a Nehalem Bay sand spit ocean beach (Figure 7A), 3) well abraded porcelain sherds (Figure 18A) and stoneware/earthenware sherd CS2024 (Figure 18C) from Smuggler Cove. Representative winter storm wind and incident wave directions are from the National Oceanic and Atmospheric Administration (NOAA) buoy 46029 (years 2015-2020) (NOAA, 2022). The diagramed 10 m-isobath (depth contour) is interpreted from the NOAA Navigation Chart 18520 (NOAA, 2004).

For this article, the alongshore artifact dispersals that took place before the 1700 great Cascadia earthquake are based on beeswax blocks, timbers, and porcelain sherds that are associated with recognized 1700 tsunami deposits or rockslide burials (Figure 17A). The alongshore dispersal time is taken to be 6 years between the loss and initial breakup of the Santo Cristo de Burgos galleon (1693–1694) and the January 1700 earthquake and tsunami inundations (Satake et al., 1996). The precise mechanisms and timings of shipwreck breakup(s) are not known. The dispersal distances are measured from a shoreline position taken due west of the sherd SC2023 site (Figure 7 and Figure 17A). The annually normalized alongshore dispersal rates of the Beeswax Wreck artifacts, prior to the 1700 tsunami surges, are 1) timbers (1.7 km yr^{-1}), 2) beeswax blocks (1.0 km yr^{-1}), and 3) ceramic sherds (0.1 km yr^{-1}). These dispersal rates represent minimum rates, as unknown artifacts could have reached further distances from the sherd SC2023 position prior to the 1700 tsunami emplacements or rockslide burial than the distances presented here. In any case, the estimated high rates of shipwreck flotsam dispersal by wind and wave stress (Figure 17A) could help to explain the relatively small proportion of shipwreck timber recovery, which is

estimated to be less than five percent of the total mass of the galleon and timber cargo (see Section 2 for timber salvage estimate).

5.2 Post-1700 Tsunami Bedload Artifact Distributions

Ceramic sherds have been collected from the ocean beaches, Nehalem Bay sand spit, and bayside shorelines in modern time (Figure 17B and Figure 18). The largest proportion (68%) of porcelain sherds in the Dubè collection (Lally, 2008; Lally, 2016) come from the Smuggler Cove (Figure 17B). Only three sherds are reported from shorelines located north of Cape Falcon, which bounds the small Smuggler Cove to the north. Considering the likely area of porcelain sherd sources from south of Smuggler Cove, the alongshore differences in the proportion of modern sherd abundances bear further examination. Burial of sherds in nearshore sand deposits along the Nehalem Bay sand spit presumably occurred shortly after 1) the breakup of the Beeswax Wreck, 2) the 1700 tsunami backwash surges over the spit, and 3) catastrophic beach retreat following the 1700 coseismic subsidence (Figure 15). The catastrophic beach retreat resulted from the transfer of beach sand to the offshore areas (10–30 m water depth) (Peterson et al., 2020), as previously discussed in Section 4.4. Ceramic fragments could have been transported offshore and buried at shallow depths in the offshore sand deposits, resulting from accommodation space filling after coseismic subsidence (Bruun, 1988; Peterson et al., 2020). Episodic vertical mixing (~1.4 m sub-bottom depth) by storm surf (Peterson & Walczak, 2022) and shoreward displacement of the innermost-shelf sand, following intersiemic uplift in historic time (Bruun, 1988; Cruikshank & Peterson, 2017) could have remobilized some buried sherds, such as sherd SB2010, as shown in Figure 17B and Figure 18B. Such remobilization could then permit storm driven northward transport in the nearshore. Another source of sherds could have been located closer to Smuggler Cove, possibly from a drifted wreck structure or cargo crates located on the south side of the Neahkahnie headland (Astoria Daily Budget, 1894). The most distal source of sherds could be from the lower Nehalem Bay, as transported down the Nehalem Bay channel and then out through the tidal inlet to the ocean nearshore and beach zones. In any case, the historic supply of well abraded sherds to Smuggler Cove requires specific transport processes to 1) bypass sherds around the Neahkahnie headland, but 2) not bypass sherds around Cape Falcon, which bounds Smuggler Cove to the north (Figure 17B).

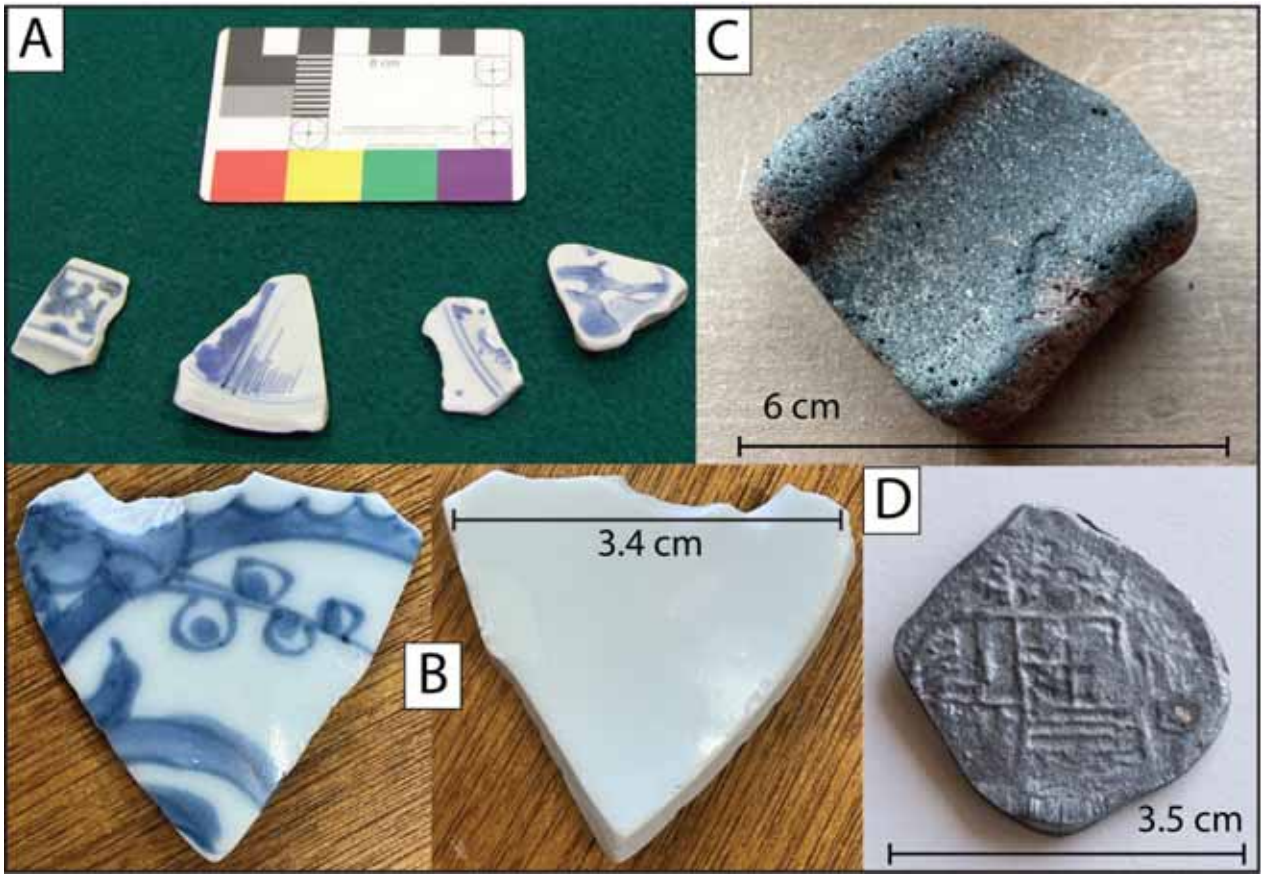

Figure 18. Scaled photographs of bedload artifacts recently collected from the study area beaches

Part A, photograph of representative abraded porcelain sherds (average width ~1.5 cm) from Smuggler Cove (Figure 17B), as archived in the Dubè collection at the Columbia River Maritime Museum, Astoria, Oregon (upper scale card 1 cm intervals). Part B, slightly abraded porcelain sherd (SB2010, 3.4 cm width) collected (2010) by Joseph Luckeroth, Beaverton, Oregon, from a modern beach (wet sand) on the seaward side of the Nehalem Bay sand spit (Figure 7). Part C, large (6 cm) stoneware/earthenware sherd (CS2024) recently collected (2024) by one of these authors (Whiting) from Smuggler Cove. Part D, abraded Spanish silver coin from a storm cobble berm at the southwest end of the Neahkahnie headland, as photographed (2022) by staff at the Nehalem Valley Historical Society Museum, Manzanita, Oregon.

A Spanish silver coin (Budde-Jones, 2004) was recently collected (2022) from a gravel berm, located just south of the Neahkahnie headland (Figure 17B and Figure 18D). The coin has rounded edges and eroded face engravings. The density of the silver coin (~9 g cm^{-3}) puts the coin close to the hydraulic equivalence of the storm wave deposited gravel. The beach gravel accumulates on the southside of the Neahkahnie headland, due to changing shoreline angles and opposing incident wave alongshore transport, as diagrammed in Figure 17B. In contrast, ceramic sherds with much lower density (~2.3 g cm^{-3}) have bypassed the Neahkahnie headland to reach Smuggler Cove. Unlike the slightly abraded porcelain sherd SB2010 (Figure 18B) that was collected from a modern beach on the seaward side of the Nehalem Bay sand spit (Figure 7), the porcelain sherds collected from Smuggler Cove are dominantly abraded (Figure 18A) (John Dubè, pers. comm., 2024). The substantial abrasion is evident by rounded corners, rounded edges, and eroded glazes. The substantial abrasion of the Smuggler Cove sherds resulted from prolonged transport in the surf zone. The minimal abrasion of the Nehalem Bay spit beach sherd (SB2010) suggests 1) recent remobilization by vertical mixing from storm wave scour and 2) negligible alongshore transport in the surf zone since very-recent vertical remobilization to sand surface. During major winter storms, northward directed wind-stress geostrophic bottom currents and wave oscillatory resuspension (Figure 17B) transport littoral sand in the nearshore (0–10 m depth) and therefore around both the Neahkahnie and Cape Falcon headlands (Peterson et al., 2020). Ceramic sherds also bypassed the gradually reoriented 5–10 m isobaths around the Neahkahnie headland to reach Smuggler Cove (Figure 17B). Storm lag gravel beds (5–10 cm thickness) have recently been documented in modern inner-shelf sand deposits to 19 m water depth, in an Oregon wave-energy testing locality (Peterson & Walczak, 2022). In contrast to the northwest trending 10-m isobath located on the south side of the Neahkahnie headland, the 10-m isobath trends due west on the south side of Cape Falcon. The sharp inflection (~90°) of the 10-m isobath at the Cape Falcon headland likely traps the north-bound sherds in the Smuggler Cove embayment. Asymmetric wave transport then delivers the well abraded sherds to the Smuggler Cove shorelines. In summary, littoral sand bypasses Cape Falcon to the north, yet this appears not to be the case with the porcelain sherds, which have accumulated in Smuggler Cove for several centuries.

A very-large and very-well abraded earthenware/stoneware sherd, collected from Smuggler Cove (CS2024 in Figure 18C), likely experienced a similar transport history of rounding the Neahkahnie headland (Litzenberg, 2022). Its transport, however, presumably occurred in shallower water depths and at corresponding higher wave/bottom current energies than the smaller porcelain sherds (Figure 18A). The reported differences in collected sherd abundances between the open ocean beaches and the Smuggler Cove beach (Lally, 2008; Lally, 2016; Litzenberg, 2022) are attributed to 1) short residence times and low concentrations of sherds exposed in the broad ocean beaches relative to 2) long residence times and high concentrations of sherds trapped in the narrow confines of Smuggler Cove. Furthermore, the favorable sherd collection conditions in Smuggler Cove might have disproportionately attracted collectors to that location, resulting in some bias in the reported sherd abundance data (John Dubè, pers. comm., 2024). Due to dangerous wave and surge conditions, no underwater searches for sherds have been conducted directly offshore of the Neahkahnie headland itself (Figure 17B). It is not known whether sherds have been sourced or concentrated in the turbulent water beneath the headland's vertical sea cliffs, interconnected sea caves, and sea stack pinnacles.

5.3 Preservation of Recovered Beeswax Wreck Artifacts

In this section, several interrelations in the study area are presented to account for the preservation of recovered flotsam artifacts from the Beeswax Wreck (Williams et al., 2018). These relations include 1) study area geomorphic conditions, 2) tsunami runup remobilization and deposition, and 3) beach, dune, and wetland burial. For example, the 1700 tsunami surges remobilized shipwreck beeswax, timbers, crates, and sherds from the study area nearshore zone and beaches to more landward positions. The low gradients of the Manzanita beach sand ramps (Figure 14) and the low elevations of the Nehalem Bay sand spit (Figure 7) permitted substantial tsunami incursions, to positions located well landward of subsequent beach erosion (Figure 15). The protected positions of the tsunami deposited artifacts afforded long-term preservation of the artifacts, as further enhanced by eventual burial under prograde beach and transgressive dune deposits. The surface areas of potential artifact deposition and

preservation along the Manzanita beaches (15 hectares) and across the Nehalem Bay sand spit (204 hectares) are shown in Figure 19A. Due to localized dune cover of tsunami strandline deposits in both the Manzanita beaches and at the ends of the Nehalem Bay sand spit, some site-specific subsurface testing is required to establish the depth of the pre-1700 surface/paleosol and the tsunami runup artifacts still located in those areas. Shipwreck artifacts remain to be discovered under dune cover along the back edges of the Manzanita beaches and across the full extent of the Nehalem Bay sand spit.

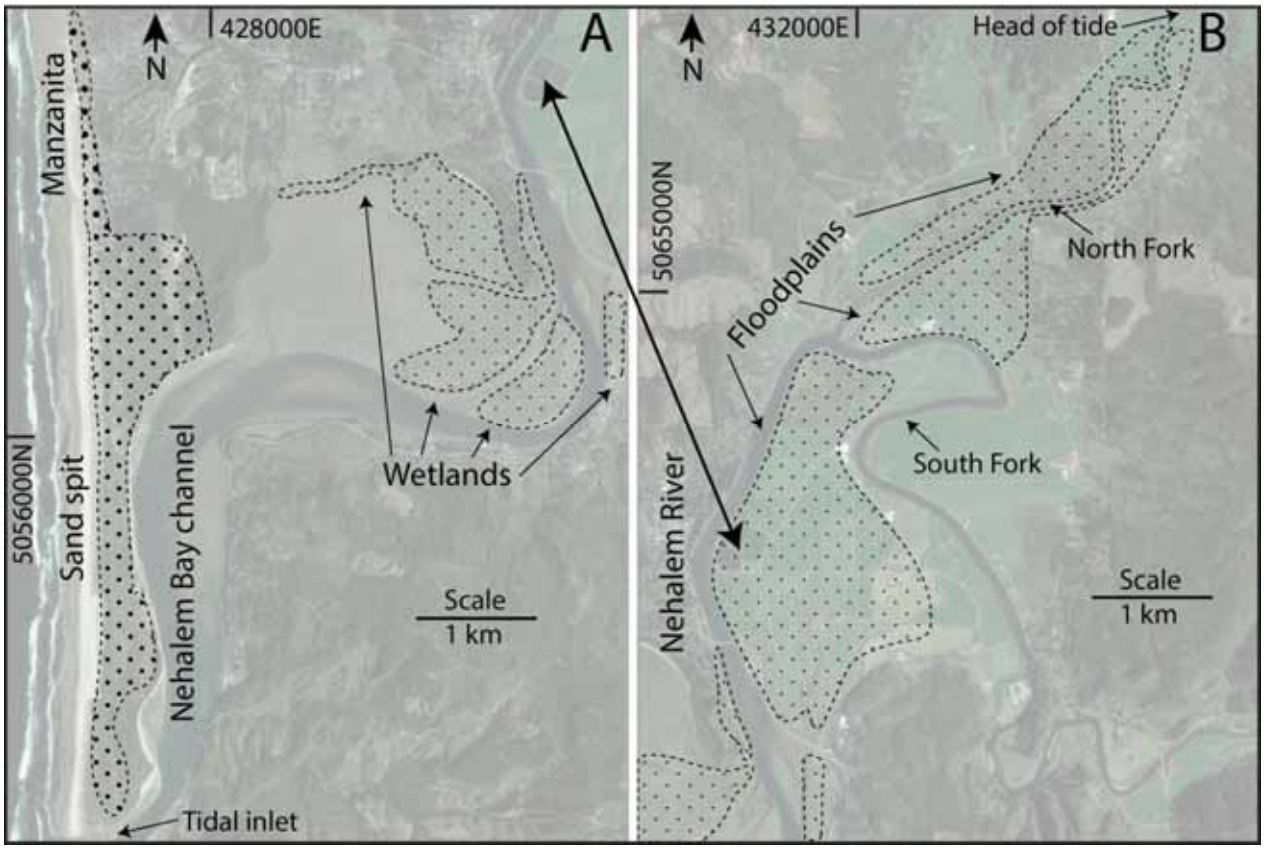

Figure 19. Maps of the potential areas of shipwreck artifact dispersal and burial protection in the study area

Part A, map of protected tsunami strandline areas at the Manzanita beaches (Manzanita), the Nehalem Bay sand spit (Sand spit), and the lower Nehalem Bay marginal wetlands (Wetlands). Base map from Google Earth Pro (Google Earth, 2024). Part B, map of protected tsunami strandline areas in the upper bay fluvial-tidal floodplains (Floodplains). The protected Manzanita beach backshore/sand ramp area is bounded by the 130 m-beach retreat scarp and the modern 10–12 m sand ramp elevations. The protected Nehalem Bay sand spit area is bounded by the 130 m-beach retreat scarp, maximum ~8 m dune elevations (north and south ends), and the bay shoreline. The protected Nehalem Bay wetlands and fluvial-tidal floodplains are bounded by bay mud flats, channel banks and modern wetland/floodplain elevations of 2.0±1.0 m NAVD88.

Protected tsunami strandline areas in the Nehalem Bay wetlands and fluvial-tidal floodplains (Figure 19) are predicted on the bases of 1) the measured elevations of 1700 tsunami strandline deposits (Figure 11), 2) subsurface depths of 1700 tsunami layers (0.3–1.0 m depth), and 3) modern surface elevations of recovered beeswax artifacts (Figure 16A). Coseismic subsidence of the Nehalem Bay wetlands/floodplains, and any overlying flotsam artifacts, was followed by peaty mud burial, thus preserving potential flotsam artifacts from oxidative biogenic decay. The combined surface areas of potential artifact preservation in the Nehalem Bay wetlands (191 hectares) and fluvial-tidal floodplains (507 hectares) are shown in Figure 19. Due to artifact dispersal across the vegetated wetlands and broad floodplains, the concentration of flotsam artifacts could diminish with increased landward distances up-river and away from major channel banks. Nevertheless, some preserved flotsam artifacts are still likely to be discovered beneath shallow mud and peat deposits in the broad Nehalem Bay wetlands.

5.4 Geomorphic and Oceanographic Comparisons of Three West Coast Galleon Shipwreck Localities

Three reported shipwrecked Spanish galleons, the Santo Cristo de Burgos (1693) near Manzanita Oregon), the San Agustín (1595) in Drakes Bay, California, and the San Juanillo (1578) near Playa Esmeralda, in the Baja California Peninsula, Mexico (Figure 1A and Figure 20) shared similar building materials, construction methods, and some bulk cargo items. Though intact ship hulls or ship deck structures have not been found in the three shipwreck localities, different abundances of shipwreck flotsam, ceramic sherds, and metal objects were distributed and subsequently collected along their respective beaches (Table 3). Ship timbers and flotsam cargo artifacts from the wrecked galleons San Agustín and San Juanillo are nearly absent. By comparison, very abundant beeswax and timber flotsam from the Santo Cristo de Burgos shipwreck (Beeswax Wreck) were salvaged for commercial purposes in the late 1800s and early 1900s (Headlight-Herald; 1921; Williams et al., 2018). Using the least traveled large metal objects and least abraded sherds, respectively, archaeologists have postulated approximate wreck site positions for the San Juanillo galleon (Von der Porten, 2023) and the San Agustín galleon (Russell, 2023). In this article, we propose a primary locality for the Beeswax Wreck breakup on the Nehalem Bay sand spit, although additional archaeological evidence is needed to constrain the specific site or sites.

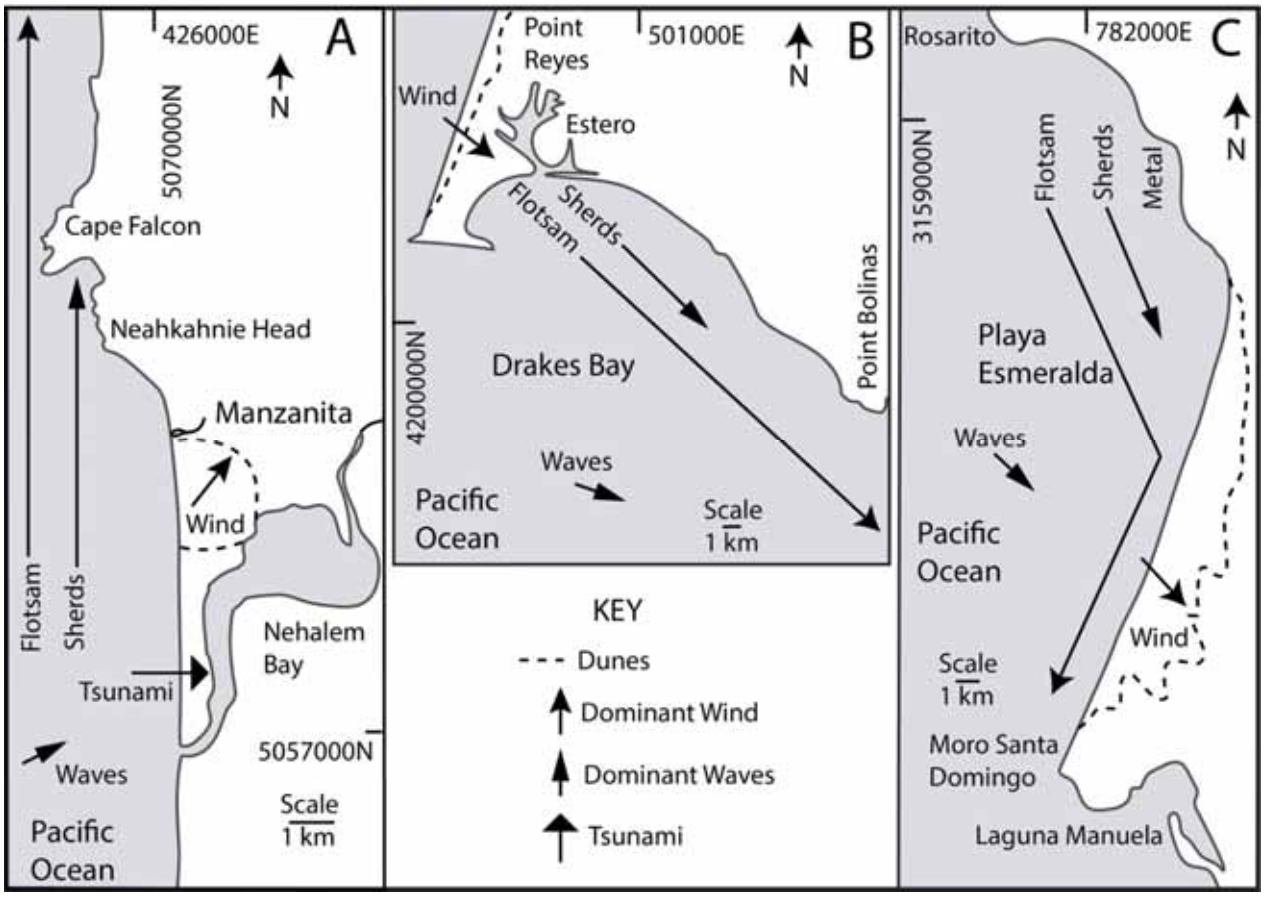

Figure 20. Galleon shipwreck localities in the central West Coast of North America

Diagrams of 1) known Spanish galleon shipwreck settings, 2) dominant wind and wave directions affecting those settings, and 3) artifact dispersals in the Beeswax Wreck locality, near Manzanita, Oregon in Part A, the San Agustín shipwreck locality in Drakes Bay, California, USA in Part B, and the San Juanillo shipwreck locality near Esmeralda, Baja California Peninsula, Mexico in Part C. The interpreted net directions of shipwreck flotsam and sherd transports are shown (arrows). Dune fields (dashed lines) demonstrate dominant wind directions from dune alignments and net littoral transport directions towards bounding headlands. Deepwater storm wave data are summarized from offshore buoys. The three galleon shipwreck localities are shown in Figure 1A.

Table 3. Reported abundances of collected shipwreck artifacts from three lost galleon localities on the west coast of North America

Galleon	Beeswax	Timbers	Ceramic sherds	Metal artifacts
Santo Christo de Burgos	6-20 tons	>10 tons	1,600	1 Chain, fittings
San Agustín	0	0	2,200	Iron spikes
San Juanillo	3 blocks	0	2,100	58

Notes: Estimated abundances of beeswax recovered from the Santo Christo de Burgos or Beeswax Wreck locality are from Williams et al. (2018). Estimated timber recovery (minimum salvage estimate) is based on one family's report of salvaged 'teak' timber haulage (1 ton) from a 1 km coastline length as extrapolated to the entire 10 km study area coastline length (see Section 2). Ceramic sherds are from the Dubè collection (Lally, 2008; Lally, 2016). Reported metal artifacts, including one copper chain and iron fittings in wood were found in the Nehalem Bay sand spit (Rogers, 1899). In the San Agustín shipwreck locality, two-thirds of the ceramic sherds and several metal spikes were recovered in Native American village and midden sites (Russell, 2023). No beeswax blocks were recovered in the San Agustín shipwreck area and no ship's cargo manifest exists for the San Agustin eastbound voyage (Matthew Russell, pers, comm., 2024). So, whether the San Agustin carried beeswax cargo is uncertain. However, beeswax was a common trade item on eastbound galleons during the period of the San Agustin's shipwreck (Von der Porten, 2019). Three beeswax blocks were recovered from the San Juanillo shipwreck locality (Junco, 2016). Sherds from the San Juanillo locality, as recovered by Von der Porten (2019), were tallied by Litzenberg (2022). Metal artifacts from the San Juanillo shipwreck locality were found 300–800 m landward from the beach in low-elevation dune deflation hollows, using a metal detector (Von der Porten, 2023).

There are important similarities and differences in geomorphologies and oceanographic conditions between the three galleon shipwreck localities (Figure 20). All three shipwrecks occurred in high wind- and wave-energy mesotidal sandy coastlines. The beaches are dominated by seasonally shore-oblique onshore winds and complementary shore-oblique wave incidence angles, as diagramed in Figure 20. Modest storm surge runup, of up to 1.0–1.5 m, occurs in the Beeswax Wreck and San Agustín shipwreck localities (Pittock, et al., 1982; Bromirski, et al., 2017). But storm surge runups in the San Juanillo shipwreck locality might reach three times those modest heights, due to weakening typhoons/hurricanes that infrequently reach the Baja California Peninsula. In all three North American West Coast shipwreck localities, the wreck debris could have been widely dispersed or lost from the shipwreck sites by alongshore transport (Figure 20). However, in the Beeswax Wreck locality, the flotsam artifacts were remobilized and transported landward by the 1700 nearfield tsunami surges, within just a few years after the shipwreck breakup. In the San Agustín locality, Native Americans manually transported some of the recovered ceramic sherds to village and midden sites (Russell, 2023). However, sherds buried in offshore sand deposits of Drakes Bay continue to be remobilized by storm waves to replenish some sherd supply to the modern beaches (Russell, 2023). In the San Juanillo shipwreck locality, metal artifacts were transported landward of the exposed beaches by large storm surge(s) sometime after the shipwreck breakup (Junco, 2016). Those artifacts are locally found in deflation hollows between dune hummocks (Von der Porten, 2023).

The near absence of flotsam artifacts in the San Agustín and San Juanillo shipwreck localities (Table 3) is attributed 1) the losses of those artifacts from the shipwreck sites before extreme storm surge or manual transport could have transferred the flotsam artifacts landward for long term protection and/or 2) a lack of substantial dune sand cover in those settings to deeply bury and preserve the stranded flotsam artifacts from oxidative biogenic decay. However, the much smaller rates of alongshore sherd dispersal (Figure 17A) permitted some sherd retention in all three shipwreck localities. As discussed above, the extraordinary abundance of flotsam artifact preservation in the Beeswax Wreck locality (Table 3) is attributed to the limited initial alongshore dispersal of artifacts, followed by the landward remobilization of shipwreck artifacts by nearfield tsunami surges within just a few years of the Beeswax Wreck breakup. The disproportionate abundance of porcelain sherds in the small Smuggler Cove locality, 68% of the Dubè collection of 1600 sherds (Table 3) (Lally, 2008; Lally, 2016) in the study area is generally attributed to 1) the long-term remobilization and northward dispersal of the ceramic sherds in the nearshore zone until 2) effective sherd catchment and retention south of the Cape Falcon headland (Figure 17B). Such headland bounded catchments of concentrated sherds are not reported for the San Agustín and San Juanillo shipwreck areas.

6. Conclusions

The fate of the lost Santo Cristo de Burgos Spanish galleon or Beeswax Wreck (1693) on the coast of northern Oregon is a rapid breakup followed by alongshore and across-shore dispersals of shipwreck artifacts in the high-energy beach settings and low elevation estuary wetlands. The Beeswax Wreck locality was impacted by 1) nearfield (1700) tsunami surges shortly after the shipwreck breakup and initial alongshore dispersal of shipwreck artifacts, and 2) catastrophic beach retreat following prolonged coastal subsidence or sea level rise after the megathrust rupture. Shipwreck beeswax blocks were used to target the 1700 tsunami runup elevations in a Manzanita beach barrage pond and in a fluvial floodplain in the upper reaches of Nehalem Bay. The floodplain tsunami elevations were substantially diminished from those recorded in the proximal beach barrage pond setting. The measured tsunami runup elevations are used to predict potential sites of tsunami transported artifacts that were deposited beyond the reach of subsequent ocean beach erosion and river channel bank erosion. Historically reported shipwreck structures confirm the extent of catastrophic beach retreat features located landward of the study area beaches. The extraordinary preservation of beeswax and wood artifacts from the Beeswax Wreck are attributed to relations of 1) rapid vessel breakup and initial dispersal of shipwreck flotsam, 2) nearfield tsunami remobilization and onshore/inshore deposition of flotsam artifacts, and 3) burial of deposited artifacts by beach sand progradation, dune sand burial, or peaty mud accumulation in their respective coastal settings. Although an intact hull of the Santo Cristo de Burgos no longer exists, the demise of this 17th century galleon continues to deliver widely-dispersed- and well-preserved artifacts to historical geographers, maritime archaeologists, and coastal geomorphologists studying the Beeswax Wreck.

Acknowledgements

John Dubè assisted with fieldwork and provided background on decades of porcelain and earthenware sherd collection in the study area, including the Nehalem Bay sand spit and Smuggler Cove. Giorgio Litt provided GPS position coordinates for the marker posts that identified the historic shipwreck structure site (Camp) on the Nehalem Bay sand spit. Jeff Smith provided access to, and assisted with, photography and measurement of the Beeswax Wreck timber and porcelain sherds, collected in Smuggler Cove, and curated at the Columbia River Maritime Museum, Astoria, Oregon. Tom Cambell assisted with the photography of the stamped beeswax block from the Nehalem Valley Historical Society Museum. Joseph Luckeroth provided access to and background information on a porcelain sherd collected from a beach on the Nehalem Bay sand spit. Dennis Woodward loaned a large beeswax block from the North Fork of the Nehalem River to the Nehalem Valley Historical Society Museum. Doug Firstbrook assisted with providing access to the Nehalem Watershed Trust properties at the Bayside Gardens wetlands, Manzanita. Access to the Doris Hassler Davis Pond wetlands was permitted by the Portland Wetlands Conservancy. Kennett Peterson provided editing support for early versions of this article.

References

Astoria Daily Budget. (1894). *Ancient Wreckage Ashore*. April 21, 1894 (p. 1).

Beals, H. K., & Steele, H. (1981). Chinese porcelains from site 35-TI-1, Netarts sand spit, Tillamook County Oregon. *University of Oregon Anthropological Papers, 23*. Portland. University of Oregon.

Birkeland, P. W. (1999). *Soils and Geomorphology*. Oxford University Press, New York.

Bromirski, P. D., Flick, R. E., & Miller, A. J. (2017). Storm surge along the Pacific coast of North America. *Journal of Geophysical Research: Oceans, 122*, 441-457. https://doi.org/10.1002/2016JC012178

Bruun, P. (1962). Sea-level rise as a cause of shore erosion. *Journal of the Waterways and Harbors Division, 88*, 117-132. https://doi.org/10.1061/JWHEAU.0000252

Bruun, P. (1988). The Bruun rule of erosion by sea-level rise: A discussion on large-scale two-and three-dimensional usages. *Journal of Coastal Research, 4*, 627-648.

Budde-Jones, K. T. (2004). Coins of the Lost Galleons. *Printing-Action Graphics,* Winter Park, Florida. 25 p.

Chambliss, W., Lehman, M., Stansbeary, A., Motola, K., Hickerson, L., & Peterson, C. (2012). Entrainment forces measured on the largest boulder transported by the last Cascadia earthquake paleotsunami (1700 CE), Nehalem Spit, Manzanita, Oregon, USA. *Oregon Academy of Sciences,* Portland, Oregon.

Clarke, S. A. (1899). Wrecked Beeswax and Buried Treasure*. Oregon Native Son, Native Son Publishing Co., Portland, OR., I*(5), 245-249.

CNN. (2022). *Centuries-old shipwreck thought to have inspired 'The Goonies' has been discovered off Oregon coast*. Retrieved from https://www.cnn.com/2022/07/26/world/goonies-shipwreck-oregon-discovery-scn/index.html

Cooper, W. S. (1958). Coastal sand dunes of Oregon and Washington. *Geological Society of America Memoir, 72*. New York: Geological Society of America. https://doi.org/10.1130/MEM72-p1

Cooper Borge, L. V. (1975). Tillamook, Oregon Thursday July 8, 1926, Bronze Handles Found at Neahkahnie. In *Tillamook History Sequel to Tillamook Memories*. Tillamook County Pioneer Association. Pg 81.

Cruikshank, K. M., & Peterson, C. D. (2017). Late-stage interseismic strain interval, Cascadia subduction zone margin, USA and Canada. *Open Journal of Earthquake Research, 6*, 1-34. https://doi.org/10.4236/ojer.2017.61001

DOGAMI. (2023). *Lidar Interactive Map.* Department of Geology and Mineral Resources. Retrieved from https://www.oregongeology.org/lidar/. Accessed January 12, 2023.

DOGAMI. (2024). *Lidar Interactive Map.* Department of Geology and Mineral Resources. Retrieved from https://www.oregongeology.org/lidar/. Accessed May 5, 2024.

Erlandson, J., Losey, R., & Peterson, N. (2001). *Early maritime contact on the northern Oregon coast: Some notes on the 17th century Nehalem Beeswax ship*. In J. Younker, M. Tveskov, & D.

Erlandson, J. M., & Moss, M. L. (1999). The Systematic Use of Radiocarbon Dating in Archaeological Surveys in Coastal and Other Erosional Environments. *American Antiquity, 64*, 431-443. https://doi.org/10.2307/2694143

Gibbs, G., Mengarini, G., & Tolimie, W. F. (1970). "Tribes of Western Washington and Northwestern Oregon. Extract from Vol. 1 of "*Contributions to American Ethnology*", Washington, D.C. 1877." The Shorey Book Store, Facsimile Reproduction: Seattle. 1970.

Giesecke, E.W. (2007). *Beeswax, teak, and castaways: Searching for Oregon's lost protohistoric Asian ship*. Manzanita, OR: Nehalem Valley Historical Society.

Google Earth Pro. (2023). *Google Earth Pro 2023*. https://www.google.com/earth/. Accessed September May 5, 2023.

Grant, W. C. (1994). *Paleoseismic Evidence for Late Holocene Episodic Subsidence on the Northern Oregon Coast*. Unpublished M.S. project, University of Washington.

Headlight-Herald. (1921). "Teak From Wreck Sold About County". *Headlight-Herald,* February 22, 1921.

Hult, R. E. (1968). *Lost Mines and Treasures of the Pacific Northwest*. Portland, OR: Binford & Mort.

Junco, R. (2016). On a Manilla galleon of the 16th century: A nautical perspective. In *Early navigation in the Asia-Pacific region: A maritime archaeological perspective* (pp. 103-113). Singapore: Springer Singapore. https://doi.org/10.1007/978-981-10-0904-4_6

Lally, J. (2008). *Analysis of the Chinese Porcelain Associated with the "Beeswax Wreck," Nehalem, Oregon.* M.S. Thesis, Department of Anthropology, Central Washington University, Ellensburg, Washington.

Lally, J. (2016). Analysis of the Beeswax shipwreck porcelain collection, Oregon, USA. In *Early navigation in the Asia-Pacific region: A maritime archaeological perspective* (p. 169-194). Singapore: Springer Singapore. https://doi.org/10.1007/978-981-10-0904-4_9

La Follette, C., Deur, D., Griffin, D., & Williams, S. S. (2018). Oregon's manila galleon. *Oregon Historical Society, 119*, 151-159. https://doi.org/10.1353/ohq.2018.0061

Lewis. (Eds.). *Telling out stories: Proceedings of the fourth annual Coquille Cultural Preservation Conference* (pp. 45-53). North Bend, OR: Coquille Indian Tribe. https://doi.org/10.1353/ohq.2018.0061

Litzenberg, V. R. (2022). *Stoneware and Earthenware from the Beeswax Wreck: Classification of the Dubé Collection and Discussion of the Interpretation of the Materials in Protohistoric Sites*. M.S. Thesis, Portland State University, Portland, Oregon.

Losey, R. J. (2002). *Communities and Catastrophe: Tillamook Response to the AD 1700 Earthquake and Tsunami, Northern Oregon Coast*. Ph.D. Dissertation, University of Oregon, Eugene, Oregon.

Marshall, D. (1984). *Oregon shipwrecks*. Portland, OR: Binford & Mort.

Meniketti, M. (2023). The wreck of the galleon *San Agustin*. A case study of economics, exploration, and European development in the Pacific Rim. In: Wu, C., 2023. Scott S. Williams and Roberto Junco (Editors): *The Archaeology of Manila Galleons in the American Continent: The Wrecks of Baja California, San Agustín, and Santo Cristo de Burgos*, Springer Nature Switzerland, p. 53-63. https://doi.org/10.1007/978-3-030-71524-3_6

Minor, R., & Peterson, C. D. (2016). Multiple reoccupations after four paleotsunami inundations (0.3-1.3 ka) at a prehistoric site in the Netarts littoral cell, Northern Oregon, USA. *Geoarchaeology, 32*, 248-266. https://doi.org/10.1002/gea.21593

Moss, M., & Erlandson, J. (1995). *An Evaluation, Survey, and Dating Program for Archaeological Sites on State Lands of the Northern Oregon Coast*. Report on file, Oregon State Historic Preservation Office, Salem

Nelson, A. R, Hawkes, A. D., Sawa Y., Englehart S. E., Witter R., Grant-Waler W. C., Bradley, L., Dura T., Cahill, N., & Horton, B. (2020). Identifying the Greatest Earthquakes of the Past 2000 Years at the Nehalem River Estuary, Northern Oregon Coast, USA. *Open Quaternary, 6*, 1-30. https://doi.org/10.5334/oq.70

Niem, A. R., & Niem, W. A. (1985). *Geologic map of the Astoria Basin, Clatsop and northernmost Tillamook counties, northwest Oregon, Oil and Gas Investigation Map OGI-14, plate 1, scale 1:100,000: Portland, Oregon, Oregon Department of Geology and Mineral Industries, Map*.

NOAA. (2022). *Buoy 46029 Historical Data Download Years 2015-2020*. National Oceanic and Atmospheric Administration National Buoy Center. Published online: https://www.ndbc.noaa.gov/download_data.php?filename=46029h2015.txt.gz&dir=data/historical/stdmet/. Accessed December 7, 2022.

NOAA. (2024). *National Oceanographic and Atmospheric Administration*. Navigation Chart 18520. Published online: https://www.charts.noaa.gov/OnLineViewer/18520.shtml. Accessed February 17, 2024.

Oregon Historical Society. (2024). *Nehalem Bay State Park*. Retrieved from https://www.oregonencyclopedia.org/articles/nehalem_bay_state_park/. Acessed June 3, 2024.

OPB. (2023). *Oregon Public Broadcasting. New documentary shares the true story that inspired 'The Goonies'*. Published online: https://www.opb.org/article/2023/11/09/goonies-shipwreck-beeswax-documentary/. Acccessed May 9, 2024.

Peterson, C. D. (2024). *Use of bare earth lidar images to interpret dune features that could host Beeswax Wreck artifacts in the Manzanita dunes and Nehalem Bay sand spit*. Final Report submitted to: Maritime Archaeological Society, Astoria, Oregon, and Nehalem Valley Historical Society, Manzanita, Oregon. 23 p.

Peterson, C.D., Carver, G.A., Clague, J.J., & Cruikshank, K.M. (2015). *Maximum-recorded overland run-ups of major nearfield paleotsunamis during the past 3,000 years along the Cascadia margin, USA and Canada*. Natural Hazards, 77, 2005-2026. https://doi.org/10.1007/s11069-015-1689-7

Peterson, C. D., & Cruikshank, K. M. (2007). *Preliminary Report on Beeswax Shipwreck Field Surveys (5/07-7/07), Manzanita, Oregon*. Submitted to Beeswax Wreck Team, and Nehalem Valley Historical Society, Manzanita, Oregon. 25 p

Peterson, C. D., & Cruikshank, K. M. (2014). Quaternary tectonic deformation, Holocene paleoseismicity, and modern strain in the unusually-wide coupled zone of the central Cascadia margin, Washington and Oregon, USA and British Columbia, Canada. *Journal of Geography and Geology, 6*(3), 1. https://doi.org/10.5539/jgg.v6n2p1

Peterson, C. D., Cruikshank, K. M., Jol, H. M., & Schilichting, R. B. (2008). Minimum runup heights of paleotsunami from evidence of sand ridge overtopping at Cannon Beach, Oregon, Central Cascadia Margin, USA, *Journal of Sedimentary Research, 78*, 390-409. https://doi.org/10.2110/jsr.2008.044

Peterson, C.D., Doyle, D.L., Rosenfeld, C.L., & Kingen, K.E.P. (2020). Predicted responses of beaches, bays, and inner-shelf sand supplies to potential sea level rise (0.5-1.0 m) in three small littoral subcells in the high-wave-energy Northern Oregon Coast, USA. *Journal of Geography and Geology, 12*, 1-27. https://doi.org/10.5539/jgg.v12n2p1

Peterson, C. D., Stock, E., Hart, R., Percy, D., Hostetler, S. W., & Knott, J. R. (2009). Holocene coastal dune fields used as indicators of net littoral transport: West Coast, USA. *Geomorphology, 116*, 115-134. https://doi.org/10.1016/j.geomorph.2009.10.013

Peterson, C., Stock, E., Cloyd, C., Beckstrand, D., Clough, C., Erlandson, J., Hart, R., Murillo- Jiménez, Percy, D., Price, D., Reckendorf, F., & Vanderburgh, S. (2006). Dating and morphostratigraphy of coastal dune sheets from the central west coast of North America. *Oregon Sea Grant Publications,* Corvallis, Oregon, 81 p. PDF on CD.

Peterson, C. D., & Walczak, M. (2022). Recent transport and deposition of littoral sand across the inner-shelf of Central Oregon: further constraints on estimating depths of closure (30–34 m) during future sea level rise in the Pacific Northwest Region, USA. *Journal of Geography and Geology, 14*(22). doi: 10.5539/jgg.v14n2p1. https://doi.org/10.5539/jgg.v14n2p1

Peterson, C. D., Williams, S., & Andes, C. (2023). Cascadia earthquake-triggered rockslide burial of Beeswax galleon wreck timbers in a sea cliff wave-cut platform site, North Smuggler Cove, Oregon, USA. *Journal of Geography and Geology, 15*(1). Published online. https://doi.org/10.5539/jgg.v15n1p1

Peterson, C. D., Williams, S. S., Cruikshank, K. M., & Duprè J. R. (2011). Geoarchaeology of the Nehalem Spit: redistribution of Beeswax Galleon Wreck debris by Cascadia earthquake and paleotsunami (~ AD 1700), Oregon, USA. *Journal of Geoarchaeology, 26*, 219-244. https://doi.org/10.1002/gea.20349

Pittock, H. L., Gilbert, W. E., Huyer, A., & Smith, R. L. (1982). *Observations of sea level, wind and atmospheric pressure at Newport, Oregon, 1967–1980*. Data Report Reference 82-12. Corvallis, OR: Oregon State University, School of Oceanography.

Reckendorf, F., Peterson, C. D., Jol. H., Vanderburgh, S., Phipps, J., Twichell, D., & Baker, D. (2003). *Holocene coastal processes in the Columbia River Littoral Cell: Pacific County, Washington and Clatsop County, Oregon*. Northwest Cell Friends of the Pleistocene, Annual Field Trip Guide, 208 p.

Rogers, T. (1899). "Beeswax Wreck is found". *McMinnnville Telephone-Register Guard*. 21 September, 1899.

Russell, M. A. (2023). The search for the San Agustín: National Park Service Investigations in Drakes Bay, Point Reyes National Seashore. In: Wu, C., 2023. Scott S. Williams and Roberto Junco (Editors): *The Archaeology of Manila Galleons in the American Continent: The Wrecks of Baja California, San Agustín, and Santo Cristo de Burgos (Oregon)* Springer Nature Switzerland, p. 65-75. https://doi.org/10.1007/978-3-030-71524-3_7

Satake, K., Shimazaki, K., Tsuji, Y., & Ueda, K. (1996). Time and size of giant earthquake in Cascadia inferred from Japanese tsunami records of January 1700. *Nature, 378*, 246-249. https://doi.org/10.1038/379246a0

Scheans, D., & Stenger, A. (1990). *Letter report: 35-TI-1A and related porcelains*. Ms. on file, Oregon State Historic Preservation Office, Salem.

Smith, S. B. (1899). Beginnings in Oregon. *The Quarterly of the Oregon Historical Society, 4*(1900), 72-97.

Swan, J. G. (1857). *The Northwest Coast; Or, three Years' Residence in Washington Territory*. University of Washington Press, Seattle and London (Sixth printing, 1998).

Von der Porten, P. A. (2019). Ghost galleon. The discovery and archaeology of the *San Juanillo* on the shores of Baja California. *Texas A&M University Press*. Texas.

Von der Porter, P. A. (2023). Metal detecting on the Baja California galleon wreck. In: Wu, C., 2023. Scott S. Williams and Roberto Junco (Editors): *The Archaeology of Manila Galleons in the American Continent: The Wrecks of Baja California, San Agustín, and Santo Cristo de Burgos* OR Springer Nature Switzerland, p. 31-39. https://doi.org/10.1007/978-3-030-71524-3_4

Vaughn, W. N. (2004). Till Broad Daylight: A History of Early Settlement In Oregon's Tillamook County. *Bear Creek Press*. Wallowa, OR. 2004.

Williams, S. S. (2007). *Research Design to Conduct Archaeological Investigations at the Site of the "Beeswax Wreck" of Nehalem Bay, Tillamook County, Oregon*. Report on file at Oregon State Parks and Oregon State Historic Preservation Office, Salem, OR

Williams, S. S. (2017). The Beeswax Wreck, a Manilia Galleon on the North Coast. *Alaska Journal of Anthropology, 15*, 79-87.

Williams, S. S. (2023). The Beeswax Wreck project: The first 14 years. In: Wu, C., 2023. Scott S. Williams and Roberto Junco (Editors): *The Archaeology of Manila Galleons in the American Continent: The Wrecks of Baja California, San Agustín, and Santo Cristo de Burgos* (Oregon) Springer Nature Switzerland, p. 77–85. https://doi.org/10.1007/978-3-030-71524-3_8

Williams, S., & Junco, R. (2023). Lost on lonely shores. The Manila galleon wrecks of North America. In: Wu, C., 2023. Scott S. Williams and Roberto Junco (Editors): *The Archaeology of Manila Galleons in the American Continent: The Wrecks of Baja California, San Agustín, and Santo Cristo de Burgos* (Oregon) Springer Nature Switzerland, p. 1-5. https://doi.org/10.1007/978-3-030-71524-3_1

Williams, S. S., Marken, M., & Peterson, C. D. (2017). Tsunami and salvage: the archaeological landscape of the Beeswax Wreck, Oregon. In A. Caparaso (ed). *Formation Processes of Maritime Archaelogical Landscapes, When The Land Meets The Sea,* Springer International Publishing, Cham, Switzerland, p 141-161. https://doi.org/10.1007/978-3-319-48787-8_1

Williams, S. S., & Peterson, C. D. (2017). *Report of archaeological testing of magnetic anomalies at the Nehalem Airstrip, Tillamook County, Oregon*. OR SHPO Report, 25 p.

Williams, S. S., Peterson, C. D., Marken, M., & Rogers, R. (2018). The Beeswax Wreck. Special Issue Oregon's Manila Galleon. *Oregon Historical Society, 119*, 192-209. https://doi.org/10.1353/ohq.2018.0049

Williams, S. S., & Von der Porten, P. A. (2018). The Manila galleon wreck of Baja California. In: Wu, C., 2023. Scott S. Williams and Roberto Junco (Editors): *The Archaeology of Manila Galleons in the American Continent: The Wrecks of Baja California, San Agustín, and Santo Cristo de Burgos* OR Springer Nature Switzerland, p. 25-29. https://doi.org/10.1007/978-3-030-71524-3_3

Woxell, L. K. (1998). *Prehistoric Beach Accretion Rates and Long-term Response to Sediment Depletion in the Columbia River littoral cell*. M.S. Thesis, Portland State University, Portland, Oregon.

Copyrights

Copyright for this article is retained by the author(s), with first publication rights granted to the journal.

This is an open-access article distributed under the terms and conditions of the Creative Commons Attribution license (http://creativecommons.org/licenses/by/4.0/).